



DEGREE PROJECT,
DEGREE PROGRAMME IN CIVIL ENGINEERING AND
URBAN MANAGEMENT
CIVIL AND ARCHITECTURAL ENGINEERING
MASTER OF SCIENCE, 30 CREDITS, SECOND LEVEL
*STOCKHOLM,
SWEDEN 2017*

Modelling of Heat Transfer for Convection-boosted Flat Vertical Radiator Surfaces

An investigation of how heat transfer is influenced by radiator height
and freestream air velocity

Oskar Scheibe

Master of Science thesis

Title	Modelling of Heat Transfer for Convection-boosted Flat Vertical Radiator Surfaces: An investigation of how heat transfer is influenced by radiator height and freestream air velocity
Author(s)	Oskar Scheibe
Department	Division of Fluid and Climate Technology
Master Thesis number	TRITA-STKL 2017:02
Archive number	
Supervisor	Adnan Ploskić, Sture Holmberg
Keywords	Heat transfer, flat vertical plate, non-isothermal, temperature profile, radiator, energy efficiency

Abstract

In this thesis, a calculation model is created to study a theoretical radiator-like configuration, consisting of a flat vertical plate heated with a constant capacity rate. This lumped capacitance model is partly created to more theoretically look at radiators with add-on-fans, but also to in such a setting look at fundamental heat transfer relationships. System heat transfer is studied for various heights, H (m), and freestream velocities, u (m/s). These results are then subject to validation, where comparison is made with values derived from two relevant reference studies.

It is found that polynomial fits well describe the results obtained from calculation. The relationships for heat transfer Q (W), heat flux q (W/m²) thus become:

$$Q(H, u) = a_{00} + a_{01}u + a_{10}H + a_{11}Hu + a_{02}u^2 \quad (\text{W})$$

$$q(H, u) = \frac{Q}{H} = a_{00}H^{-1} + a_{01}H^{-1}u + a_{10} + a_{11}u + a_{02}H^{-1}u^2 \quad (\text{W/m}^2)$$

For these relationships, polynomial coefficients a_{00} , a_{01} , a_{10} , a_{11} and a_{02} are found for three temperature set-ups of system supply and return temperature at zero freestream velocity: 55/45, 45/35 and 35/25 (°C). These values are chosen as they correspond to standard temperatures for low-temperature heating set-ups.

Model validation is successful for the case of natural convection ($u = 0$), whereas difficulties are encountered for the cases of mixed and forced convection. Reasons for these difficulties are discussed and it is concluded that there is a need for more experimental studies of flat vertical plates with non-isothermal wall temperature profiles.

Sammanfattning

Detta examensarbete består av att en beräkningsmodell byggts upp avsedd för att närmare undersöka en särskild teoretisk konstruktion, lik rumsradiatorer, bestående av en plan vertikal platta uppvärmd av ett konstant termiskt flöde. Denna modell består av hoplänkade element (en. *lumped capacitance*) som skapas dels för att utifrån ett mer teoretiskt perspektiv studera rumsradiatorer med elementfläktar, och dels för att i ett sådant sammanhang närmare undersöka grundläggande förhållanden avseende värmeöverföring. Den värmeöverföring som uppstår mellan systemet och dess omgivning undersöks för olika höjder, H (m), och friströmshastigheter, u (m/s). Resultaten genomgår sedan en valideringsprocess, vari de jämförs med resultat från beräkningar baserade på två referensstudier.

Det framkommer att polynom kan användas för att väl beskriva resultatet från beräkningarna. För den totala värmeöverföringen Q (W) och värmeflödet q (W/m^2) presenteras förhållandena:

$$Q(H, u) = a_{00} + a_{01}u + a_{10}H + a_{11}Hu + a_{02}u^2 \quad (\text{W})$$

$$q(H, u) = \frac{Q}{H} = a_{00}H^{-1} + a_{01}H^{-1}u + a_{10} + a_{11}u + a_{02}H^{-1}u^2 \quad (\text{W}/\text{m}^2)$$

För dessa förhållanden beräknas polynomkoefficienterna a_{00} , a_{01} , a_{10} , a_{11} and a_{02} för tre olika temperaturinställningar, med olika framlednings- och returtemperatur för systemet för det fall friströmshastigheten är noll: 55/45, 45/35 and 35/25 ($^{\circ}\text{C}$). Dessa värden motsvarar vanliga temperaturer i lågtemperatursystem.

Modellen kan till fullo valideras i fallet med naturlig konvektion ($u = 0$), men svårigheter uppstår vid validering i fallet med forcerad och blandad konvektion. Möjliga orsaker till dessa svårigheter diskuteras med slutsatsen att det finns ett behov av fler experimentella studier för plana vertikala plattor med en icke-konstant temperaturprofil i höjddled.

Contents

Nomenclature.....	1
Variables.....	1
1. Introduction.....	3
1.1 Background.....	3
1.2 Motivation of study and limitations.....	4
1.3 Problem statement.....	6
2. Method.....	7
2.1 Basic model considerations.....	7
2.2 Calculation set-up.....	10
2.3 Equations used.....	13
2.4 Calculations for Case A.....	18
2.5 Validation for Case A.....	19
2.6 Calculations for Case B.....	20
2.7 Validation for Case B.....	21
2.8 Curve-fitting and data processing.....	22
3. Results.....	24
3.1 Introduction.....	24
3.2 Total heat transfer and heat flux.....	24
3.3 Validation of results.....	25
3.4 Additional results concerning the 2002 reference study.....	28
4 Discussion.....	31
4.1 Final results.....	31
4.2 Calculation method.....	31
4.3 Validation.....	31
4.4 Further comments.....	32
5 Conclusion.....	33
6 Future Work.....	34
7 References.....	35
Appendix A.....	37
A.1 Main code.....	37
A.2 Functions.....	41

Nomenclature

Variables

Latin letters

A	(m ²)	Plate area
\mathbf{a}	(-)	Vector of polynomial fit coefficients a_{ij}
C	(W/K)	Heat capacity rate in radiator
c_p	(J/kgK)	Specific heat capacity of liquid heating radiator surface
g	(m/s ²)	Gravitational acceleration
Gr	(-)	Grashof number
H	(m)	Plate height
H'	(-)	Constant from universal function in reference study
h	(W/m ² K)	Heat transfer coefficient
\dot{m}	(kg/s)	Mass flow of radiator fluid heating radiator surface
n	(-)	Number of calculation cells
Nu	(-)	Nusselt number
Pr	(-)	Prandtl number
Q	(W)	Heat transfer
R^2	(-)	Coefficient of determination
Ra	(-)	Rayleigh number
Re	(-)	Reynolds number
Ri	(-)	Richardson number
S	(K/cm)	Linear temperature gradient over plate height
T_∞	(K)	Freestream temperature
T_f	(K)	Film temperature – average of plate and freestream temperatures
T_{LMTD}	(K)	Logarithmic mean temperature difference
T_m	(K)	Mean temperature of radiator and radiative surfaces in room
T_{ret}	(K)	Fluid temperature exiting radiator
T_{sup}	(K)	Fluid temperature entering radiator
T_w	(K)	Wall temperature, i.e. temperature of vertical flat plate
u_∞	(m/s)	Freestream velocity
w	(m)	Plate width
y	(m)	Distance from below along height of plate

Greek letters

α	(m ² /s)	Thermal diffusivity of air
β	(1/K)	Thermal expansion coefficient of air
ΔT	(K)	Temperature drop along radiator surface
ε	(-)	Emissivity
η	(-)	Constant from parameter for universal functions in reference study
θ'_0	(-)	Constant from universal function in reference study
θ'_1	(-)	Constant from universal function in reference study
θ'_{00}	(-)	Constant from universal function in reference study
λ	(W/mK)	Thermal conductivity of air
λ_0	(-)	Factor depending on temperature distribution in reference study
λ_1	(-)	Factor depending on temperature distribution in reference study
ν	(m ² /s)	Kinematic viscosity of air
σ	(W/m ² K ⁴)	Stefan-Boltzmann constant

Subscripts

55/45	Related to temperature configuration 55/45 °C (supply/return temperature)
45/35	Related to temperatures configuration 45/35 °C (supply/return temperature)
35/25	Related to temperatures configuration 35/25 °C (supply/return temperature)
acc	Accumulated
av	Average
cell	Value for a calculation cell along surface
con	Convective
iso	Isothermal
mid	Middle of cell
rad	Radiative
w	Wall
y	Distance along the plate height

1. Introduction

The aim of this study is to establish the relationship between, on one hand, the heat flux along one dimension from the surface of a radiator, and on the other hand, the surrounding freestream air velocity and the radiator height. Today, room radiators are by far the most commonly used heating devices in Swedish homes. For enhanced energy efficiency, a lower supply temperature is preferable – a method commonly known as Low Temperature Heating. This is beneficial for the efficiency of a range of heat sources, among them district heating and heat pumps. Low Temperature Heating is improved by add-on-fans, increasing the air velocity along the radiator.

In this study, a calculation model is developed and its results validated against literature values. As is seen, there is little literature and experimental work done for this particular case of heat transfer. This study thus has two purposes. Firstly, it establishes a theoretical relationship for the heat transfer of an increasingly important radiator configuration. Understanding such a relationship enables better system design and hence better energy efficiency. Secondly, the study casts light on the area of heat transfer along flat vertical surfaces with linear temperature profiles. As this area has not yet been thoroughly studied, this thesis contributes to filling a gap.

1.1 Background

1.1.1 Energy efficiency and indoor climate

The building sector is a large user of energy, and various measures are being taken to reduce this energy use. Globally, the energy sector represents about 30 % of the total energy use. At the current rate of development, this is expected to increase. Meanwhile, there is an increasing interest in constructing energy efficient buildings. Among other places, this can be seen in the increasing interest in green building certifications (Dodge Data & Analytics, 2016).

In Sweden, the building sector represents some 40 % of the total national energy use (Statens energimyndighet, 2015). As a member of the European Union, Sweden is to implement the Europe 2020 strategy, including the 20/20/20 goals. As part of this, the energy efficiency is to be increased by 20 % until 2020 (European Commission, 2010). Relating to this trend, the Swedish building norms have been made stricter, most recently in 2015. This has lowered the maximum allowed energy use in houses that are to be built (BBR, 2015). Also, the Swedish government has decided to focus on making older buildings more energy efficient (Fastighetsvärlden, 2015). Regardless of legislation and government policy, energy savings might also be motivated by a possible increase in energy prices.

Besides energy savings, good indoor climate is an important consideration in the building sector. One aspect of indoor climate is thermal comfort, which depends on a range of different parameters, as originally presented by P. O. Fanger (Fanger, 1970). A good indoor climate brings many advantages, ranging from an overall higher satisfaction among building occupants to better occupant health. From an economic point of view, it is noteworthy that a better indoor climate has been found to improve employee productivity (Seppänen et al, 2005). In Sweden, there are several sources of regulation on indoor climate. One of these is the national building code (BBR, 2017).

1.1.2 Fan-forced convection for radiators

To achieve demands on energy efficiency and indoor climate, various technical solutions are being implemented and considered. One area of development is in modification and enhancement of heat emission from radiators. It should be noted that the term *radiator* often is used (perhaps somewhat less formally) to describe a system with both radiative and convective heat output. Such a definition of the term will be used throughout this thesis. One technical solution used for room radiators is placing add-on-fan blowers on them. This set-up is shown in Figure 1 below. Field studies have shown that in this way the heat output of a radiator can be increased by more than 50 % (Johansson, 2011).

In general, this addition to the radiator can be successfully combined with heat pumps, in which the water supply temperature to the radiator system is decreased while maintaining an adequate radiator heat output. These so-called low-temperature systems have been found to comply with demands on indoor climate (Wang & Holmberg, 2015). A set-up with add-on-fan blowers can be beneficial for energy efficiency. For example, if the energy is supplied by a heat pump, it has been found that the heat pump COP (coefficient of performance, ratio of total heating to supplied energy) increases with decreased system temperatures (Ploskić, 2010). Also, a lower supply temperature leads to lower distribution heat losses in piping networks. This is particularly useful for the case of district heating systems, where there are potentially large heat losses due to the sometimes extensive distribution grid. Furthermore, the energy supply for the district heating itself becomes more efficient with lower temperatures, as it can more easily be combined with power production.



Figure 1. Add-on-fan placed on a single-panel radiator (elementflakten.se, 2016)

1.2 Motivation of study and limitations

For systems with add-on-fan blowers on radiators, as is shown schematically in Figure 2 below, it is interesting to know the relationship between the radiator heat output and various underlying system parameters. Several system parameters affect the heat output. In this investigation, the study of various impacting parameters will be limited to three: freestream air velocity, radiator height and water supply temperature to the radiator.

The freestream velocity largely affects the heat output and this will be more closely examined. As freestream velocity is increased, the convection mode along the radiator gradually shifts from natural to mixed and forced convection, and this increases the overall heat transfer. Radiator height is related to heat output such that an increase in the former leads to an increase in the latter. This is due to a larger heat emitting area, and also such a radiator contains a larger amount of hot water which further improves its heat transfer ability. Furthermore, the effect of water supply temperature is examined as it is currently used as the most common mean of system control. As heating loads increase, radiator heat output is normally increased by increasing the supply temperature. Also, heating systems are normally designed for some specific combination of supply and return temperature at a certain indoor temperature. It thus becomes interesting to study the effects of freestream air velocity and radiator height for various supply temperatures.

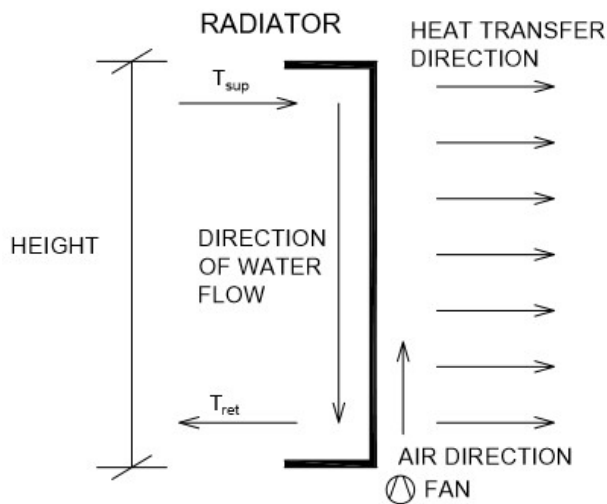


Figure 2. Schematic drawing of radiator with add-on-fan

To narrow down the scope of this investigation, a range of factors relevant to system design will not be taken into consideration. These include among many other: energy source COP or temperature-dependent efficiency (e.g. efficiency in thermal plants), height dependent freestream air velocity variation and radiator surface material. In order to produce a simplified radiator model, many such things will be ignored.

This thesis aims to produce a simplified model for a radiator system. Thus, various simplifications will be made, of which many are explained and motivated below in part 2. In this part of the essay, some basic model simplifications are further explained, as these are related to limiting the scope of this investigation.

As the heat output and temperature distribution over a radiator surface depends on the radiator design, the study is limited to only examining radiators of type 10. This is one of several different radiator types, which are shown in Figure 3 below. Such a radiator consists solely of a vertical plate and no convection fins. Commercial type 10 radiators in Sweden are rarely completely flat, but instead have some surface roughness in the shape of some pattern. This is probably largely due to aesthetic considerations, as heat transfer can be easily increased by changing radiator type – adding additional plates and/or convection fins.

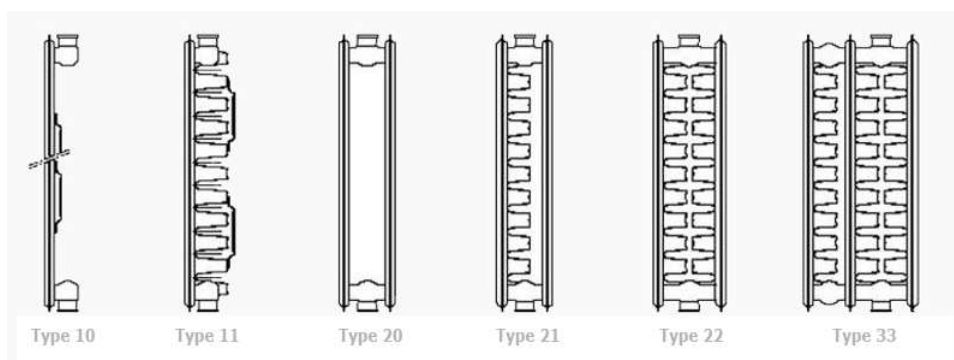


Figure 3. Profiles of radiator types (radiatoren.blogspot.se, 2017)

The topic examined in this thesis thus clearly relates to problems in heat transfer theory. To make this connection even clearer, so that the model proposed in this thesis can be compared to and validated by actual research, some further simplifications are made. One side, rather than two sides,

of the plate is considered. Also, the plate is taken to be completely flat. Finally, only changes along one dimension of the plate – the height – are considered, such that variations occur along its height while variations are neglected along its length (or, alternatively, it is seen as homogenous along its length). With these modifications made, the model becomes a one-dimensional flat vertical plate, clearly corresponding to an often considered and much examined heat transfer configuration.

From such a radiator system the heat flux (W/m^2) is perhaps what is most interesting to examine. It is obvious that total heat output increases with increased radiator height. However, as has also been seen in various contexts – among these experimental studies (Ploskić, 2010) – the heat flux decreases with radiator height. This is an advantage for systems such as baseboard skirting radiators. The extent of what advantage these systems have in terms of heat flux clearly affects their viability in system design and optimization. Heat flux is clearly of great interest in low-temperature heating (*LTH*) systems as well. Thus, results will be presented for heat flux.

Thus, in the end, the scope of this thesis becomes to for a certain heated system investigate a fundamental heat transfer problem. Historically, empirical equations have been produced for a case similar to the one studied. In more modern time, various more numerically oriented approaches have been proposed. This thesis, however, focuses on comparing model results with more analytical approaches that have been published in recent years. This is meant to validate model results, but also turns into a way of analyzing the reasonability of results derived with basis in the published studies.

1.3 Problem statement

The problem statement of this thesis is summarized in points 1) through 3) below.

- 1) Create a calculation model for the study of one side of a flat vertical plate radiator system.
- 2) Validate model results by comparing to results with empirical data from literature.
- 3) Calculate total heat transfer and heat flux as function of freestream velocity and plate height for different water supply temperature configurations.

2. Method

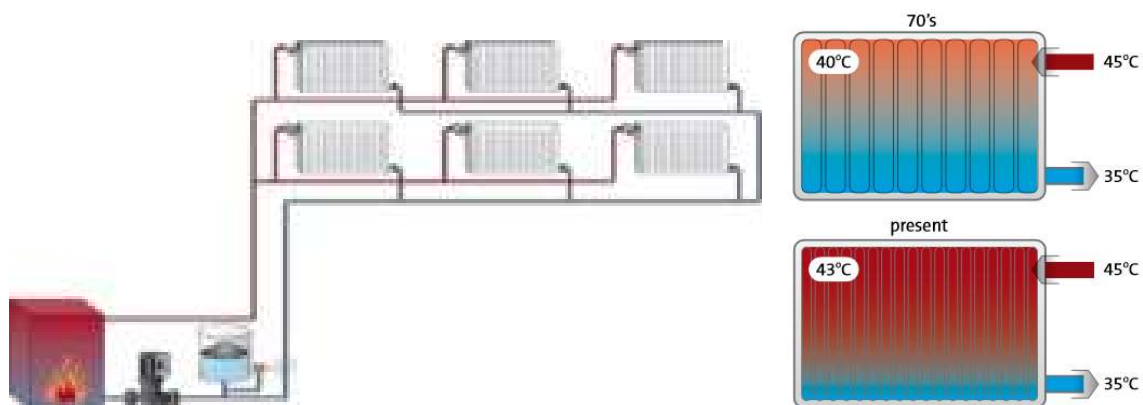
In this section, the method used for the investigation is explained. First, the basics of the calculation model created are explained. This is done continuing with limitations and generalizations as was started in the previous part of the essay. Next, the set-up for the calculations is further explained and the order of calculations is outlined. Following this, all the basic equations used are presented. Next, the major separate parts of calculations are presented individually.

To continue, the calculations used for the two cases are described – the base case of full natural convection and that where some non-zero freestream velocity is introduced. This is followed by explanations of how the calculated values are validated. The validation is based on two reference studies, one for each respective case. Comparisons are made between calculated values and values suggested by the reference studies, with the purpose to validate the calculated values. Finally, an explanation is given of how the results are processed to be presented. The calculations are made in MATLAB® and the code is presented in its entirety in Appendix A.

2.1 Basic model considerations

In this part of the thesis, the model used is further explained. First, the set-up of a modern hydronic heating system is briefly explained. Next, the various considerations of the model used are explained at greater depth.

A typical modern hydronic heating system is presented in Figure 4 below. Water is heated by some heat source, which in Figure 4 is represented by the furnace. This need not be an actual boiler, but could for example be a heat pump or district heating. Next, heated water is supplied to the system by supply pipes. In the figure, this is represented by the red pipes. Each radiator is supplied independently with heating water, which leaves the radiators in return pipes. In the figure, this is represented by the blue pipes. Before the return pipes returns to heating, it passes an air vent, an expansion tank and a pump. This shows the main parts of a hydronic heating system. At times, there are additional parts, such as a cleaning device at the right side of the pump.



Left: Figure 4. Typical two-pipe hydronic heating system (grundfos.com, 2017)

Right: Figure 5. Increasingly even temperature distribution in radiators (RADSON, 2016)

It should be noted that the system in Figure 4 is a two-pipe system. Typically, modern hydronic systems are of this type. Alternatively, some or all water passing one radiator can be used to heat the next one, in a system of radiators connected in series. This, however, is more common in older high-temperature systems. For lower-temperature systems, with reasonable radiator liquid flows, this causes too low supply temperatures for radiators later along the chain. The heat output from these radiators become too low, as the heat output of a radiator is roughly proportional to its supply

temperature. This is suggested by the fundamental relationship between heat flow and temperature difference, and has also been shown experimentally (Calisir et al, 2015).

A radiator system can be installed with different supply and return temperatures, a pair of temperature here denoted $T_{\text{sup}}/T_{\text{ret}}$. The European standard for radiators, EN 442, recommends a 10 K difference between the two temperatures (SS EN 442, 1996). This value will be used as a basis in this study. Since high-temperature systems to a large extent has lost popularity, and radiator systems successfully can be combined with lower temperatures, this study will look at the temperatures $T_{\text{sup}}/T_{\text{ret}}$ of 55/45, 45/35 and 35/25 °C.

The temperature configurations, $T_{\text{sup}}/T_{\text{ret}}$, utilized correspond to what are considered standard values for *Medium temperatures*, *Low temperatures*, and *Very Low Temperatures*, as these terms have been defined (Boerstra et al, 2000). Medium temperatures are 55/45 °C, low temperatures are 45/35 °C, and very low temperatures are 35/25 °C, according to definition.

It will be assumed that the radiator system operating with these temperatures is operating in a steady state, with a constant radiator liquid flow. This is the most common radiator system configuration. Further, it is assumed that the system is installed to operate at such conditions when no fan-assisted convection is taking place. As a fan is turned on, there will be some delay until the system reaches a new equilibrium. What time this takes will depend on several system-specific parameters. Supposedly, it is rarely a long duration. A field study on one radiator has shown a reasonably steady state achieved in less than 30 minutes (Johansson, 2011). In this thesis, only the heat transfer at steady states will be considered, as these results are of more general nature.

This study only considers a generalized case of a radiator with radiator fluid entering at its extreme top and leaving at its extreme bottom. This creates a certain temperature distribution along the radiator surface's height. Also, there is commonly a temperature distribution along the radiator's width. However, with the development of more modern radiators this difference is becoming increasingly small, according to manufacturers, as seen above in Figure 5. Motivated by this, and strive for generalization, this study's calculations are one-dimensional, only considering temperature differences along the radiator height.

Among heat transfer processes, this model considers only interactions between the plate and its surrounding. With basis in this, and starting with a generalized starting point in a linear temperature distribution (Johansson, 2011), wall temperature is calculated along the plate height by a simple iterative method later described. The plate is modelled by means of lumped system analysis. This requires a low Biot number in every node of the discretization, meaning in this case substantially larger convective than internal conductive heat transfer of the system. As radiator plates are typically very thin, and metal thermal conductivity is typically very large, this is a fairly accurate approximation. Thus for practical purposes, conduction can be ignored (Johansson, 2011).

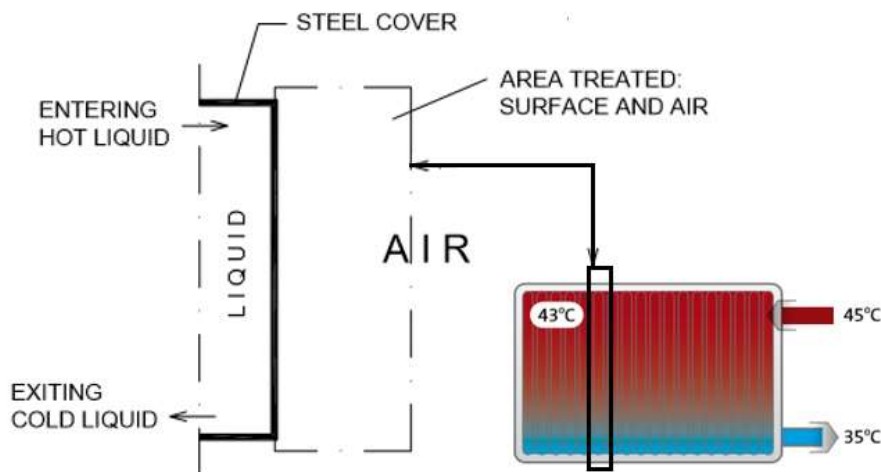


Figure 6. Limitation of area treated by model (partly (RADSON, 2016))

Only one side of the radiator is considered, better corresponding to theoretical models in this area. This is roughly equivalent to the side of a single-panel radiator directed towards a room. Such radiator types are commonly known as Type 10 (Warfvinge, 2010). Also, the freestream air velocity is taken to be constant. Such simplifications have been used for analysis of this type of radiator systems (Johansson, 2011; Jonsson & Ahlstrand, 2005). In other literature, the limitations of such a simplification have been discussed (van der Wijst, 2010). Still, it has been noted that much work in this area is based on the assumption of a constant freestream velocity, and results have been meaningful. The simplification of a constant freestream air velocity has been widely used both in studies with more mathematical treatment of heat transfer problems, as well as in more practical work. Heat transfer – even with the simplifying assumption of a constant freestream velocity – is, as later will be shown, an active area of research. For this thesis to have an adequate level of focus, it will be limited to handling only the case of constant freestream velocity.

Figure 6 above shows the limitations of the area treated by the model of this thesis. Note that this figure is partly based on Figure 5 above, and that the source (RADSON, 2016) has been used to better show the area studied. The vertical section of the radiator (although theoretically of infinitesimal width) is turned 90 degrees counterclockwise, and is shown schematically in the left part of the figure.

Throughout the thesis, two freestream air velocity options will be examined. These are: Case A, with zero freestream velocity, and Case B, with non-zero freestream velocity. As for Case A, only natural convection takes place along the plate height. For Case B, the upper region along the plate might be subject to natural convection. However, for this case there might also exist other convection modes, namely mixed and forced convection. To simplify calculations, these cases are treated separately in the following.

2.2 Calculation set-up

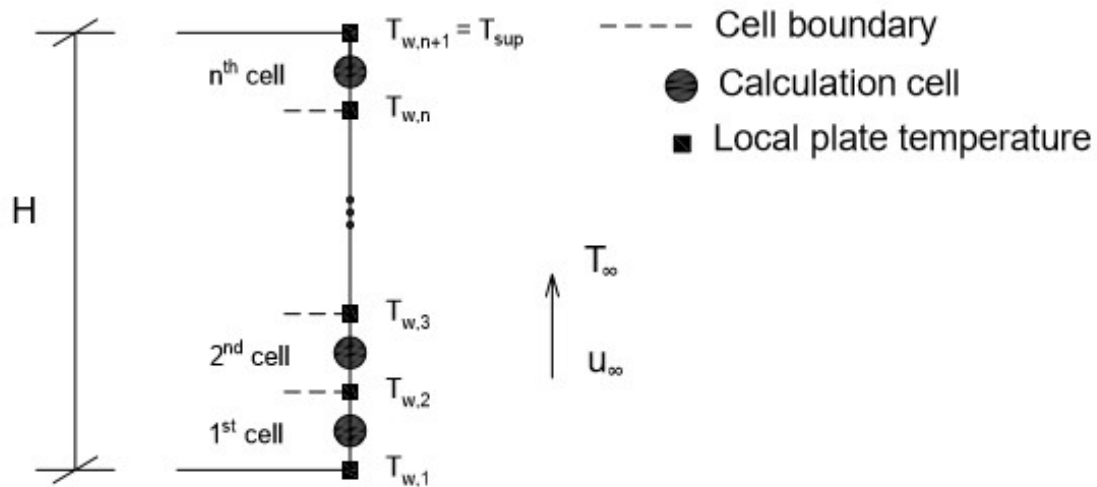


Figure 7. Schematic model of calculated case

Calculations are based on the cell model shown in Figure 7 above. The plate surface is divided into n cells. These are surrounded by a total of $n + 1$ different local plate temperatures. The uppermost temperature is defined as T_{sup} . Outside the boundary layer of the plate, there is a freestream velocity u_{∞} and temperature T_{∞} .

An overview of the calculation method is shown by the flow chart in Figure 8 below. First of all, some initial values are chosen. These include the minimum and maximum plate height H that are examined, and also the increment between such values considered. Also, the maximum freestream air velocity u_{∞} is determined, as well as the increment between values of it. Here, heights of 300 to 1000 mm will be considered. The increment is set to 10 mm, giving a total of 71 cases considered. The range of velocities considered is 0.0 to 5.0 m/s, with the increment of 0.1 m/s. This gives a total of 51 cases.

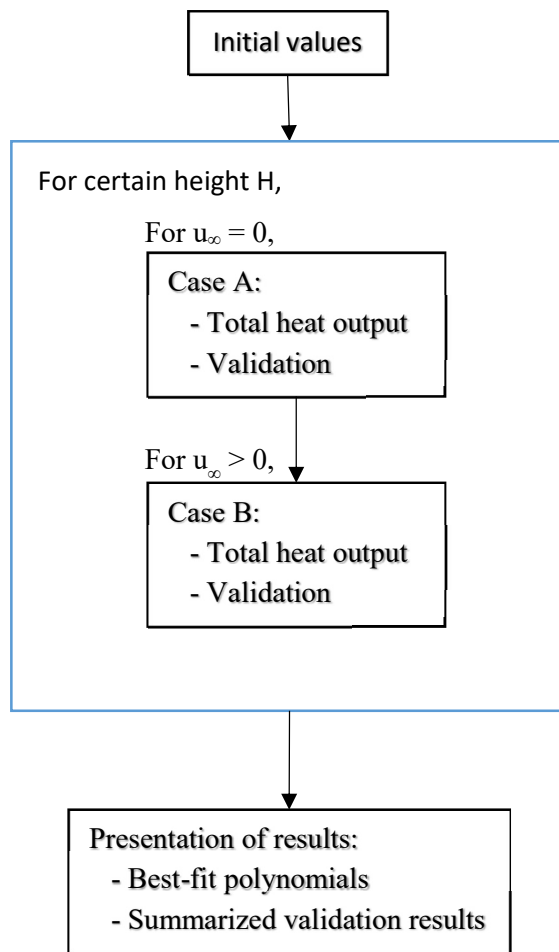


Figure 8. Overview flow chart of calculations

Other initial values include the supply and return temperatures for the base case of full natural convection, the temperature pair $T_{\text{sup}}/T_{\text{ret}}$. Note that only T_{sup} always will have constant value. As described later, T_{ret} is set to vary as the freestream velocity is increased from zero. Furthermore, the initial values include some constants listed below in Table 1.

Table 1. Some of the constants for the calculations

Variable	Value	Comment
Plate width, w	1 m	The width of the plate, arbitrary.
Stefan-Boltzmann's constant, σ	$5.67 \times 10^{-8} \text{ W/m}^2\text{K}^4$	According to literature (Holman, 2010).
Gravitational acceleration, g	9.81 m/s^2	According to literature (Holman, 2010).
Emissivity, ϵ	0.9	Common approximate value.
Freestream temperature, T_{∞}	293 K	Common indoor temperature.
Number of plate cells, n	Varying, 300 - 1000	Cells of height 1 mm.

As can be seen, the calculations are based on two for-loops. These are nested so that all freestream air velocity cases are calculated for every single height case. This gives a total of $51 \times 71 = 3621$ combinations for which calculations are made. The details of the calculations taking place for the two for-loops are presented in more detail in following sections.

Next, the results are processed. In this part, a polynomial fit is found for the gathered data points for heat output. Finally, the results from the validation calculations are processed, to better evaluate the outcome of the validation.

The heat transfer from a vertical flat plate has been studied extensively. Empirical relationships for the isothermal case were established by different authors, for example by Churchill and Chu in 1975 (Churchill & Chu, 1975). However, real results might differ from values calculated with these equations by as much as 20 % (Holman, 2010). Nevertheless, still today these empirical relationships remain the textbook cases of isothermal heat transfer from a flat vertical plate (Holman, 2010). They are widely applied practically.

The non-isothermal case, in contrast, has not been as thoroughly examined. This was noted by Havet and Blay in a 1999 article, also pointing out that the equations for the isothermal case could not be directly applied to non-isothermal cases without a loss of precision (Havet & Blay, 1999). Whereas Havet and Blay published a solution for a linear temperature distribution for the case of natural convection, a more recent study sought to give a more general solution for other types of convection. In their 2012 article, Gavara, Dutta and Seetharamu presented a method for calculating the heat transfer for an arbitrary temperature distribution in the case of forced and mixed convection (Gavara et al, 2012). Their method is based on solving the boundary layer equations by using a perturbation technique.

Instead of using the relationships presented in the two mentioned studies, this thesis will be based on another method of calculation, dividing the non-isothermal plate into several isothermal cells, as shown in Figure 7 above. To evaluate the success of such a method, comparisons will be made with the two studies presented above. Although radiation is also considered in the model, whereas the two reference studies are more focused on convection, this has a relatively small effect on the model evaluation. Because of the original inspiration of this study – the add-on-fan blower system – the physical values for air are used for the heated fluid, while the nature of the heating side is left unspecified. The heating side has some characteristics however, including a constant specific heat capacity. The general method used is applicable to other fluids with general characteristics similar to those of air.

In Table 2 below, the methods used for calculating heat transfer that have been used in this investigation are presented, showing for what case they apply. By plate temperature distribution is meant the nature of the temperature distribution along the plate. This includes the cases of constant plate temperature, a linear plate temperature distribution and the case for which it is arbitrary. It should also be noted that the freestream velocity is constant. Equations presented as for constant plate temperature are the ones used for the thesis method, as will be further presented below.

Table 2. Overview of methods and equations considered

	Freestream velocity		
	Zero	Non-zero	
Plate temperature distribution	Constant	(Churchill & Chu, 1975)	(Holman, 2010)
	Linear	(Havet & Blay, 1999)	(Unclear.)
	Arbitrary	(Gavara et al, 2012)	(Gavara et al, 2012)

The two studies presented for the linear and arbitrary cases are used for validation. For what cases these are used is further explained by Table 3 below. In this table, it is shown what reference study is used for validation for what cases that the plate model studied. In this study, the plate model will varyingly be subject to natural, mixed and forced convection. Also, for the case of natural convection, there can be multiple options for freestream air velocity. It should be noted that although the 1999 study (Havet & Blay, 1999) strictly only applies to natural convection in a case of zero freestream velocity, it is still applied to the case of natural convection in non-zero freestream velocity cases. This is to simplify the validation process. As this convection mode rarely occurs for the investigated plate heights and freestream velocity, it has only a very minor impact on later validation results.

Table 3. Overview of studies used for validation

	Freestream air velocity		
		Zero	Non-zero
Convection mode	Natural convection	(Havet & Blay, 1999)	(Havet & Blay, 1999)
	Mixed convection and forced convection	(Not occurring in case studied.)	(Gavara et al, 2012)

2.3 Equations used

In this section, all equations used are presented. First, empirical equations for calculating air properties are mentioned. Next, it is shown how cell temperatures are calculated. Following this, it is explained how values for dimensionless numbers are obtained in the calculations. With all this presented, this section proceeds to present how heat transfer is calculated. First, explanations are given for radiative heat transfer. Explanations for convective heat transfer follow. With all this done, it is explained how total heat transfer is calculated. Finally, a background is given to the calculations constituting validation of the study.

2.3.1 Air properties

The physical properties of air depend on the local temperature. As calculations are made for several different temperatures, and the plate is non-isothermal, these variations has to be taken into account.

All the values presented below apply to dry air. In reality, there is often some relative humidity. However, the relevant physical air properties do not change much because of this, and this humidity is therefore neglected. It should also be noted that values are for the normal atmospheric pressure of 1 atm.

Air properties in this setting are normally evaluated at the film temperature, being the average of the wall temperature and the freestream temperature:

$$T_f = \frac{T_w + T_\infty}{2} \quad (\text{K}) \quad (1)$$

For certain cases, other methods of variable property evaluations have been suggested (for example by Wylie (Wylie, 1973)). However, the film temperature is generally used, at least as a good approximation (Holman, 2010).

With the method used, convective heat transfer is evaluated over a certain distance, covering several calculation cells. Thus, for certain properties the average film temperature will be used, which for some cell k is:

$$T_{f,av} = \frac{1}{2} \left(\frac{1}{k} \sum_{i=1}^k T_{w,k} + T_\infty \right) \quad (\text{K}) \quad (2)$$

For the thermal conductivity, λ , the local film temperature is used. This means that it is the average temperature of only the specific cell temperature and the freestream temperature. The equation for the thermal conductivity is shown below (McQuillan et al, 1984).

$$\lambda = \frac{2.3340 \times 10^{-3} T^{3/2}}{164.54 + T} \quad (\text{W/mK}) \quad (3)$$

It should be noted that for several of these air properties, the empirical equations used do not show units of empirical constants. However, the units of the relevant air properties are stated to the right of the expressions.

For the other air properties calculated, the average film temperature is used. Among these is the thermal expansion coefficient of air, β . The expression for it is given below (Holman, 2010):

$$\beta = \frac{1}{T} \quad (1/\text{K}) \quad (4)$$

The kinematic viscosity, ν , is given by (McQuillan et al, 1984):

$$\nu = \left(\frac{2.4090 \times 10^8}{T^{3/2}} + \frac{2.6737 \times 10^{10}}{T^{5/2}} \right)^{-1} \quad (\text{m}^2/\text{s}) \quad (5)$$

The thermal diffusivity, α , is given by (McQuillan et al, 1984):

$$\alpha = (-4.3274 + 4.1190 \times 10^{-2} T + 1.5556 \times 10^{-4} T^2) \times 10^{-6} \quad (\text{m}^2/\text{s}) \quad (6)$$

2.3.2 Cell temperatures

There are n calculation cells, as shown by Figure 7 above. For every one of these, two temperature differences are calculated. First, a local temperature difference is found. This is later used for radiation heat transfer calculations, as described below. This is a temperature difference between the wall and its surroundings, calculated as logarithmic mean temperature difference (T_{LMTD}). For a cell k it becomes:

$$T_{\text{LMTD}, k} = \frac{T_{k+1} - T_k}{\ln \frac{T_{k+1} - T_\infty}{T_k - T_\infty}} \quad (\text{K}) \quad (7)$$

As convection heat transfer calculations are based on properties up to a point along the vertical plate, an alternative T_{LMTD} -value is needed. This, the accumulated T_{LMTD} for a cell k , is expressed as:

$$T_{\text{LMTD}, \text{acc}, k} = \frac{T_{k+1} - T_1}{\ln \frac{T_{k+1} - T_\infty}{T_1 - T_\infty}} \quad (\text{K}) \quad (8)$$

2.3.3 Dimensionless numbers

Based on physical constants, as well as some of the temperatures and air properties presented above, relevant dimensionless numbers can be calculated. These numbers will be presented in this section. Note that just like the air properties, these will vary along the plate height.

The Prandtl number, Pr , is also an air property. For a cell k it is given by:

$$Pr_k = \frac{\nu_k}{\alpha_k} \quad (9)$$

The Grashof number, Gr , is used for calculations for natural convection. The value of Gr partly depends on a cell's vertical position on the plate, y_k . This height corresponds to the height of the upper temperature of the cell, i. e. the height at temperature T_{k+1} for cell k . It should be noted that the temperature below, $T_{\text{LMTD}, \text{acc}, k}$, is closely corresponding to wall temperature (T_w). The expression thus becomes:

$$Gr_k = \frac{g\beta_k T_{LMTD,acc,k} y_k^3}{\nu_k^2} \quad (10)$$

The Rayleigh number, Ra, is the product of the Prandtl and the Grashof numbers, such that:

$$Ra_k = Gr_k \times Pr_k \quad (11)$$

The Reynolds number, Re, is used for calculations for forced convection. This number also depends on a cell's vertical position on the plate, y_k , such that:

$$Re_k = \frac{u y_k}{\nu_k} \quad (12)$$

Finally the Richardson number, Ri, is defined as:

$$Ri_k = \frac{Gr_k}{Re_k^2} \quad (13)$$

2.3.4 Radiative heat transfer

Radiative heat transfer is calculated for every single cell. The energy being radiated from a cell depends on the cell area. As the cell height is taken to be 1 mm, this becomes:

$$A = 0.001 \times w \text{ (m}^2\text{)} \quad (14)$$

As generalizations are made here, radiative heat transfer is calculated by a simplified method. Adapting a formula to the generalizations made here, the radiative heat transfer can be expressed as (Trüschel, 1999):

$$Q_{rad,k} = h_{rad} A T_{LMTD,k} \approx 4\varepsilon\sigma T_m^3 A T_{LMTD,k} \text{ (W)} \quad (15)$$

Here, h_{rad} is the radiative heat transfer coefficient. The factor T_m is the mean temperature of the radiator surface and the surfaces in the room. The following approximation taken from Trüschel, and adapted, is used here (Trüschel, 1999):

$$T_{m,k} = \frac{1}{2} (T_{rad,k} + T_{room \text{ surfaces}}) \approx \frac{1}{2} \left(\frac{T_{k+1} + T_k}{2} + T_\infty \right) \text{ (K)} \quad (16)$$

2.3.5 Convective heat transfer

Convective heat transfer is calculated for every single cell. The heat transfer from a cell k is expressed as:

$$Q_{con,k} = h_{con,k} A T_{LMTD,k} \text{ (W)} \quad (17)$$

The convective heat transfer coefficient, $h_{con,k}$, is given by:

$$h_{con,k} = \frac{Nu_{cell \text{ av},k} \lambda_k}{y_{mid,k}} \text{ (W/m}^2\text{K)} \quad (18)$$

The average vertical position of the cell, $y_{mid,k}$, is the average of the upper and lower bound of the cell, such that:

$$y_{mid,k} = \frac{y_{k+1} + y_k}{2} \text{ (m)} \quad (19)$$

The cell average Nusselt number, $Nu_{cell \text{ av},k}$, is obtained by comparing the average Nusselt number of the distance to the upper bound of the cell with that of the distance to the lower bound of the cell. This is expressed as:

$$Nu_{cell \text{ av},k} = \frac{Nu_{av,k+1} y_{k+1} + Nu_{av,k} y_k}{y_{k+1} - y_k} \quad (20)$$

(Holman, 2010). Consequently, Q will practically only depend on ΔT . The product of ΔT and c can be denoted B , such that:

$$Q = B\Delta T \quad (29)$$

2.3.7 Basis for validation in Case A

Natural convection calculations are validated by comparison with a reference study (Havet & Blay, 1999). The relevant findings from the reference study that are used are presented below.

The 1999 study seeks to find average Nusselt values for temperature profiles along the surface height with slope S , such that:

$$S = \frac{\Delta T_w}{\Delta y} \quad (\text{K/cm}) \quad (30)$$

Here, ΔT_w represents the temperature difference between the uppermost and lowest part of the wall. For validation purposes, only the case of $S > 0$ is relevant. The average Nusselt value of such a plate is found in relation to the average Nusselt value of an isothermal plate at the same Rayleigh number. This is similar to the case of an isothermal plate at a temperature that is the average of the linear distribution, and to simplify this case is used. The study suggests two relations, depending on Rayleigh number:

$$\frac{\text{Nu}_{av}}{\text{Nu}_{av,iso}} = 1 + 0.17S, \quad \text{if } \text{Ra} \leq 2 \times 10^9 \quad (31)$$

$$\frac{\text{Nu}_{av}}{\text{Nu}_{av,iso}} = 1 + 4.15\text{Ra}^{-0.15}S, \quad \text{if } \text{Ra} > 2 \times 10^9 \quad (32)$$

2.3.8 Basis for validation in Case B

As has earlier been stated, calculated results are validated by comparison with results calculated based on a 2012 study (Gavara et al, 2012). The most important steps of these calculations are presented below. The entire code used for calculations is presented in Appendix A.

The 2012 study proposes solutions to any type of temperature distribution along the plate. However, for this to be possible, the temperature profile needs to be expressed analytically. As the temperature distribution for regions with forced and mixed convection are generally found to correspond well to linear approximations, all cases are treated as linear. To correspond to notation used in the reference study, the temperature distribution is presented as:

$$T_w - T_\infty = my + c \quad (\text{K}) \quad (33)$$

As a contrast to notation used previously in this essay, m and c corresponds to the normal coefficients of a straight line. The reference study utilizes certain functions, λ_n , which depend on the temperature distribution (Gavara et al, 2012). These functions are related to the wall temperature distribution such that:

$$\lambda_n = \frac{y^{n+1}}{T_w - T_\infty} \frac{d^{n+1}}{dy^{n+1}} (T_w - T_\infty) \quad (34)$$

The relevant expressions of lambda are presented next:

$$\lambda_0 = \frac{my}{my+c}$$

$$\lambda_1 = 0$$

$$\lambda_0^2 = \left(\frac{my}{my+c}\right)^2$$

For some height y , the Nusselt number can then be calculated by:

$$\frac{Nu_y}{Re_y^{1/2}} = -(H'(0) + \lambda_0 \theta'_0(0) + \lambda_1 \theta'_1(0) + \dots + \lambda_0^2 \theta'_{00}(0) + \dots) \quad (35)$$

Here, the functions H , ϑ_0 , ϑ_1 and ϑ_{00} are universal functions from which universal constants are derived. These universal functions are supposedly found by solving sets of ordinary differential equations by using a fourth order Runge-Kutta method. Despite various attempts, these solutions were not successfully recreated in this thesis. This might be because the reference study was not correctly understood. It appears, however, as if not a sufficient amount of boundary conditions are stated for when a certain parameter, η , is equal to zero.

As the reference study presents values for the universal constants for several different Richardson numbers, these solutions are taken as a basis. The values considered are those for the Richardson values of 0.0 – 10.0. To determine intermediate values, cubic spline interpolation is used. Judging by the values of universal constants presented in the reference study, these seem to strongly increase or strongly decrease with respect to the value of Ri. Also, the calculated points in the reference study are given to a good numerical precision. Thus, a cubic spline fit is deemed suitable.

2.4 Calculations for Case A

The basic flowchart for the calculations of Case A are shown in Figure 9 below. Initially, the temperature distribution is set to be linear. The first temperature value, at the bottom of the surface, is set to the return temperature, while the n^{th} temperature value, i.e. the uppermost, is set to the supply temperature. Thus, the increment between every temperature point will be $(T_{\text{sup}} - T_{\text{ret}})/n$. A temperature distribution is then computed iteratively, with the Gauss-Seidel Method, as explained below.

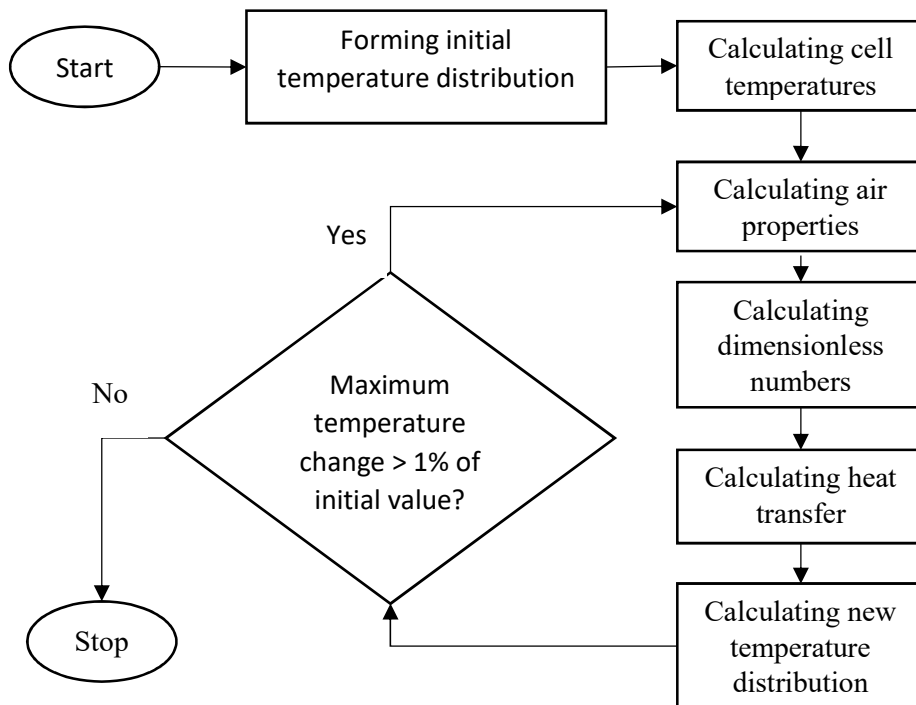


Figure 9. Calculation flowchart for Case A

The iterative cycle starts by calculating the different cell temperatures. Next, the air properties are found, after which the dimensionless numbers can be obtained. With all these figures known, all heat transfer can be computed, both radiative and convective.

After this, a new temperature distribution is computed. This is still based on the same boundary conditions, namely that the first and the n^{th} cells have fixed temperatures. The k^{th} temperature is calculated comparing the sum of the total heat transfer of the cells below the temperature point to the total heat transfer of all cells. This expression becomes:

$$T_{w,k} = T_{\text{ret}} + \frac{\sum_{i=1}^{k-1} Q_{\text{tot},i}}{\sum_{i=1}^n Q_{\text{tot},i}} \Delta T \quad (\text{K}) \quad (36)$$

Next, all these temperature values are compared to those of the earlier cycle (or in the case of the first cycle, the initial values). If every single value is found to be differing by less than 0.01, i. e. 1 %, these new values are accepted as final values.

Other values than 0.01 could be set as the requirement for minimum convergence. However, a relatively high value makes the calculations run faster, and accuracy is found to remain adequate with a value of 0.01.

2.5 Validation for Case A

Case A, later used as a base case, with only natural convection taking place, is validated by comparison with a reference study, published by Havet and Blay in 1999 (Havet & Blay, 1999). The validation processes consists of three parts, which are outlines in Table 4 below.

Table 4. Parts of the validation for Case A

Part	Purpose	Method	Result
1	Testing linearity of calculated wall temperature, T_w	Method of least squares	Coefficient of determination, R^2
2	Testing difference between wall temperature T_w and linear case	Mean absolute percentage deviation between distributions	Mean absolute percentage deviation (temperatures)
3	Comparing Nusselt number of calculated case with reference study	1) Calculating Nu according to reference study method. 2) Mean absolute percentage deviation between Nu values of thesis method and reference study	Mean absolute percentage deviation (Nu)

The main objective of the validating calculations is to compare the Nusselt number calculated by the thesis method with that of the method proposed by the 1999 study (Havet & Blay, 1999). However, as this method is based on a strictly linear temperature distribution along the wall height, comparison is first made to ensure that there is sufficient similarity between the obtained wall temperature and a linear distribution.

Thus the first part of the validation is to test the linearity of the obtained wall temperature profile. This is done using the method of least squares (*MLS*). The obtained result is the coefficient of determination, R^2 , which indicates the extent of the linearity.

The second part of the validation is meant to further test the similarity between the obtained wall temperature profile and the strictly linear profile used for calculations based on the 1999 study (Havet & Blay, 1999). Not only is linearity as such tested, but with the second validation part also the absolute percentage deviation between the temperature profiles. The result presented is the mean absolute percentage deviation (*MAPD*).

With these two validation tests made, it can be ensured that there is an overall similarity between the temperature profiles compared, so that the results can be adequately validated by the 1999 study. Possibly, a few outlier temperature points of the profile obtained might deviate from the linear fit, but the overall results can by testing potentially be found such that the 1999 study is adequate for validation purposes.

Finally, in the third part of the validation, the obtained Nusselt values are compared with the average Nusselt value calculated based on the reference study. As a basis for reference study calculations, average values for air properties and plate temperature are used, so that an average Nusselt value first can be calculated, which is later adjusted based on reference study equations. Next, a comparison can be made. Here also, *MAPD* is used as a measurement comparing Nusselt values.

2.6 Calculations for Case B

The calculations for the case with non-zero freestream velocity closely resembles those for Case A, shown in Figure 10 below. However, the initial conditions are set differently and this is further explained in the following.

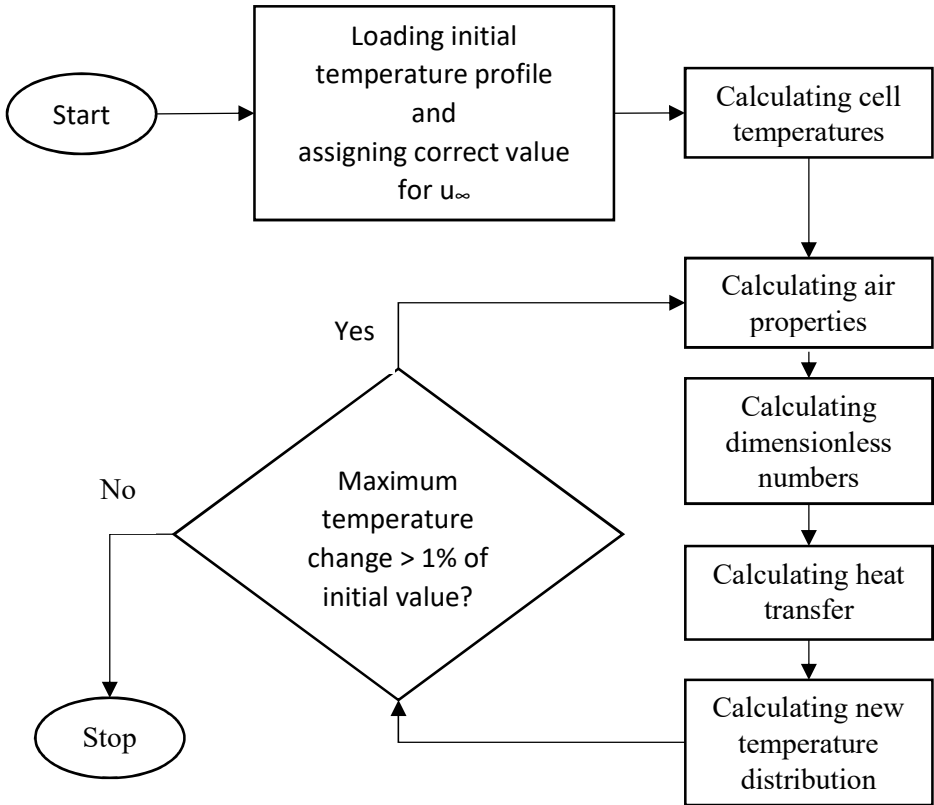


Figure 10. Calculation flowchart for Case B

Instead of a linear initial temperature distribution, these calculations start off with the final results from the previous calculations. In the case of $u_{\infty} = 0.1$, which is the lowest non-zero freestream

velocity used, this means that the base case is used. For the cases where $u_\infty = k > 0.1$, the temperature profiles for respective cases of $u_\infty = k - 0.1$ are used.

The other main difference between calculations for Case A and Case B is in how the new temperature distribution is calculated. The first temperature value along the wall height, which is at the bottom of the wall ($y = 0$), is left to float instead of being set constant. This means that T_{ret} also floats, and that ΔT increases to values larger than 10 K. In the iteration cycle of the calculations, a new return temperature is found before the temperature distribution is updated. This new return temperature is calculated based on the constant thermal mass flow B from Case A, such that:

$$T_{ret} = T_{sup} - \frac{\sum_{k=1}^n Q_{tot,k}}{B} \quad (\text{K}) \quad (37)$$

With this return temperature used as the first temperature value along the height, the temperature distribution can be updated in the same manner as for Case A.

2.7 Validation for Case B

Validation for Case B, the case with non-zero freestream velocity, is more complex than for Case A. The reason for this is partly that heat transfer along the wall can occur in all convection regimes. In Figure 11 below, a possible distribution of characteristics of convection is shown. It should be noted that the figure is schematic, and actual heights along which convection occurs in certain regimes largely can differ from what is shown in the figure. It will eventually be seen that for most values of u_∞ used, there will not be any natural convection at all along the wall. Furthermore, Ri is shown to increase along the y -direction. Further demonstrating this relationship is outside the scope of this investigation.

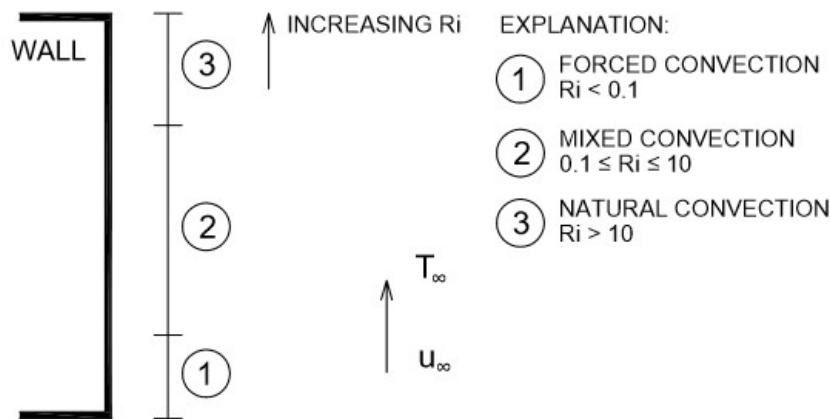


Figure 11. Possible convection regimes along wall height for Case B

In Figure 11 above, the wall is divided into three regions (1 – 3) depending on convection regimes. To validate the results, the regions are divided into two sections, the first section containing region 1 and 2 and the second section containing region 3. During the validation, the border between the two sections is first found. Next, each section is validated independently. Like for Case A, the validation consists of various parts, which are outlined in Table 5 below.

Table 5. Parts of the validation for Case B

Part	Region	Purpose	Method	Result
1	1 and 2	Testing linearity of calculated wall temperature, T_w , of region 1 and 2	Method of least squares	Coefficient of determination, R^2
2	1 and 2	Comparing Nusselt number of region 1 and 2 with reference study	1) Calculating Nu according to reference study method. 2) Mean absolute percentage deviation between Nu values of thesis method and reference study (Gavara et al, 2012)	Mean absolute percentage deviation (Nu)
3	3	Testing linearity of calculated wall temperature, T_w , of region 3	Method of least squares	Coefficient of determination, R^2
4	3	Comparing Nusselt number of region 3 with reference study	1) Calculating Nu according to reference study method 2) Mean absolute percentage deviation between Nu values of thesis method and reference study (Havet & Blay, 1999)	Mean absolute percentage deviation (Nu)

For regions 1 and 2, the same reference study is used (Gavara et al, 2012). As calculations based on the 2012 study require an analytical expression of the temperature distribution along the wall height, it is first found how well the temperature profile obtained corresponds to such an expression – namely a linear relationship. During the working process, creating the validation procedure, other analytical relationships were considered for describing the temperature profile, such as a logarithmic fit. However, it was quickly found that a linear fit yields the best results. Thus, it is first tried to what extent the obtained values correspond to a linear temperature profile. Next, the calculated Nusselt values are compared to those calculated based on the 2012 study (Gavara et al, 2012), and the result is presented in terms of MAPD value.

Region 3, with natural convection, is validated by a similar method to that which the entire wall is validated for Case A. Here, a minor simplification is made. No MAPD is calculated comparing the calculated temperature points with those of a linear distribution. Other than that, the validation process is the same.

2.8 Curve-fitting and data processing

Finally, the heat transfer data generated is processed so that conclusions can be drawn. First of all, the relationship between total heat output Q , plate height H and freestream velocity u is found. This relationship is presented for better visualization. It also shows that results indeed have a form that could have been anticipated. These results are presented by a surface, corresponding to a polynomial fit. Also, the coefficient of determination for this polynomial fit, R^2 , is presented. The polynomial is an expression of the first order of H and the second order of u , containing as well a cross-product term. This has the form:

$$Q(H, u) = a_{00} + a_{01}u + a_{10}H + a_{11}Hu + a_{02}u^2 \quad (\text{W}) \quad (38)$$

The coefficients a_{ij} are denoted:

$$\mathbf{a} = (a_{00}, a_{01}, a_{10}, a_{11}, a_{02}).$$

To achieve the most important results, a polynomial is found for the corresponding relationship for the heat flux q . This is also presented as a surface. Since the width is set to 1 m, this relationship becomes the polynomial function for total heat output divided by the height. Thus, this function is obtained as:

$$q(H, u) = \frac{Q}{H} = a_{00}H^{-1} + a_{01}H^{-1}u + a_{10} + a_{11}u + a_{02}H^{-1}u^2 \quad (\text{W/m}^2) \quad (39)$$

Next, all data obtained from the validation calculations is presented. All categories of relevant values are presented separately. The maximum and minimum values are presented, and also the mean value and the standard deviation of values.

3. Results

3.1 Introduction

In this section, the results of the calculations previously described are presented. As three sets of supply and return temperatures ($T_{\text{sup}}/T_{\text{ret}}$) were considered, three different results are presented for every variable. Different subscripts are used to present the results for the different temperature sets: 55/45, 45/35 and 35/25.

3.2 Total heat transfer and heat flux

The total heat transfer from the plate set-ups examined are presented in Figure 12 below.

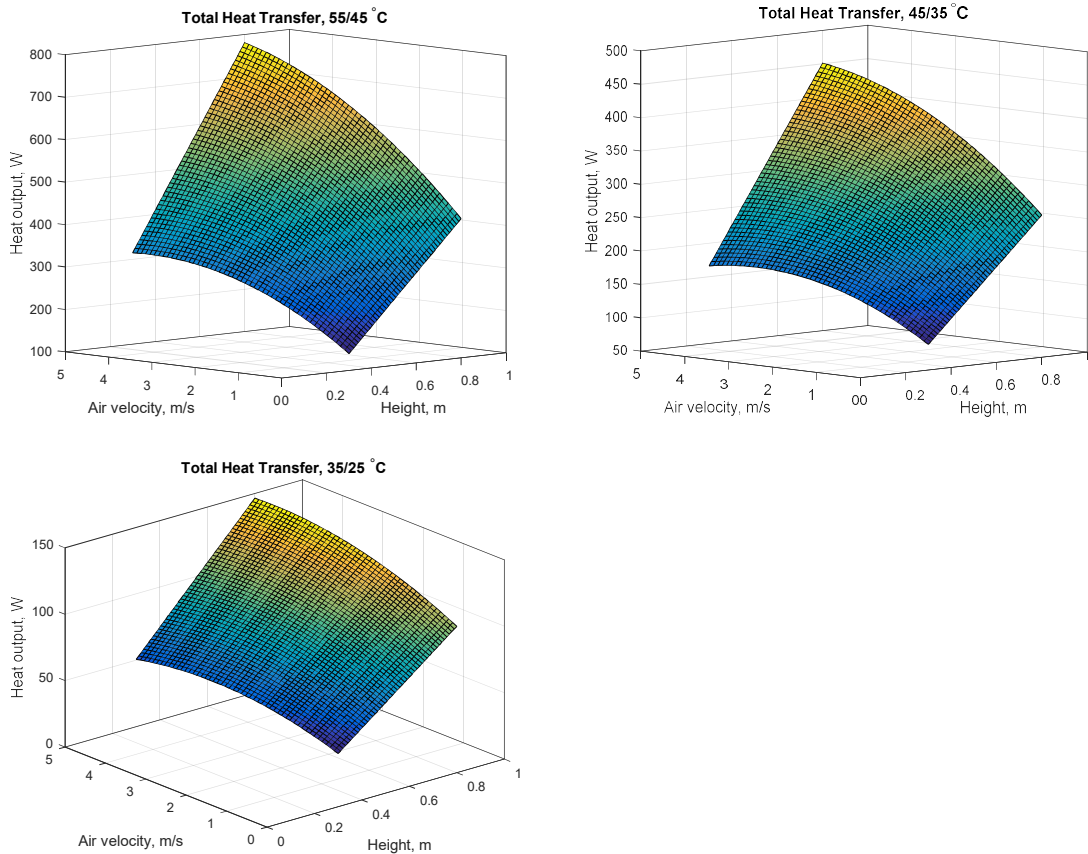


Figure 12. Total heat transfer for the width of 1.0 m at the different temperature set-ups

For the polynomial for total heat output, $Q(H,u)$, as well as for that of heat flux, $q(H,u)$, the coefficients for the different temperatures are approximately:

$$\mathbf{a}_{55/45} = (-33.37, 576.8, 55.48, 70.80, -8.313),$$

$$\mathbf{a}_{45/35} = (-16.98, 350.0, 30.11, 43.87, -5.525),$$

$$\mathbf{a}_{35/25} = (-2.197, 140.4, 7.864, 10.20, -1.754).$$

These polynomials fit the values with coefficients of determination as shown below:

$$R_{55/45}^2 = 0.9977,$$

$$R_{45/35}^2 = 0.9953,$$

$$R_{35/25}^2 = 0.9929.$$

Based on these values, the heat flux can be found. This is presented in Figure 13 below.

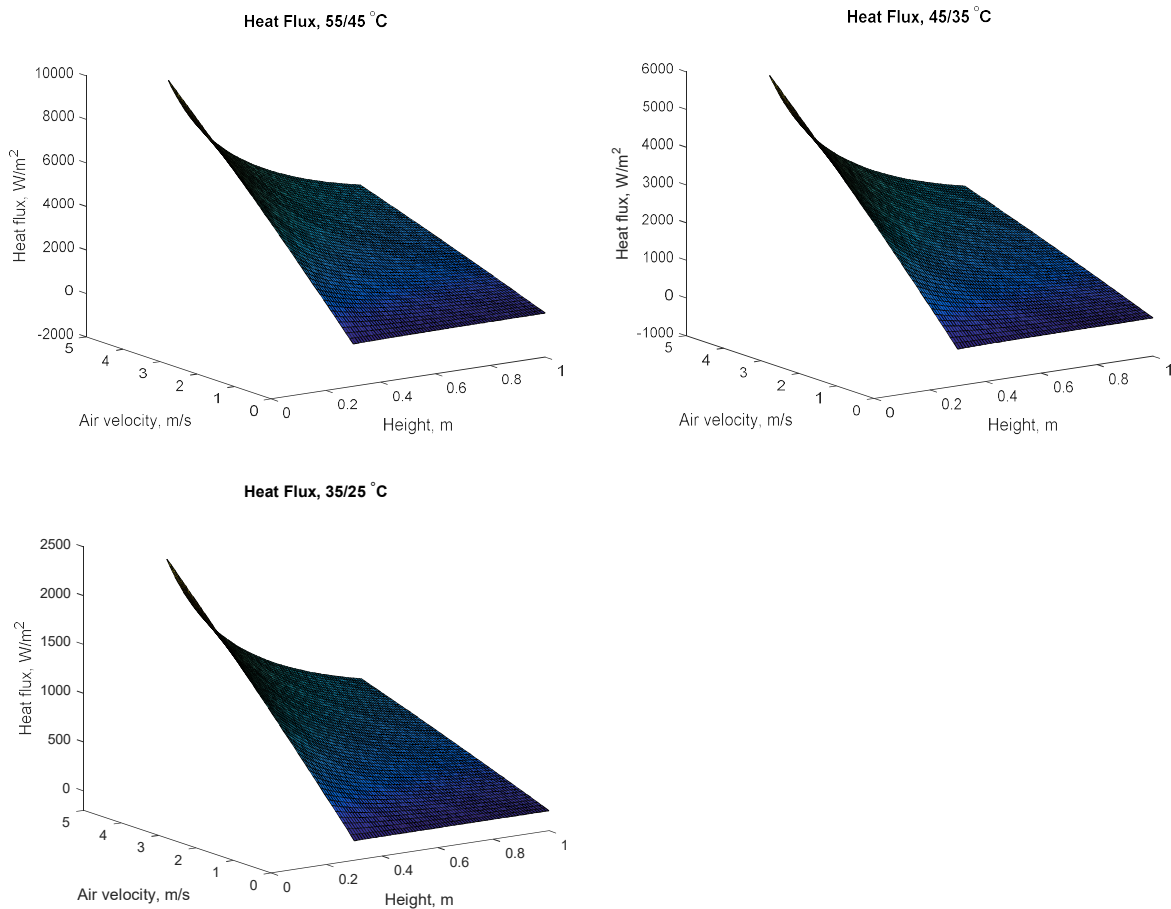


Figure 13. Heat flux at the different temperature set-ups

3.3 Validation of results

In the following two sections, the results from the validation process are presented. First, the values for Case A (the case with full natural convection) are presented. Next, the validation results for Case B (the cases with combined convection types) are presented. For every case, every validation part, as presented above, is presented separately and in the same order.

3.3.1 Validation results for Case A

For the case of full natural convection, the results for Part 1, linear approximation of the calculated wall temperature distributions, are presented in Table 6 below.

Table 6. Results for validation of Case A, Part 1

Temperature set	Maximum R^2	Minimum R^2	Mean of R^2	Standard deviation of R^2
55/45 °C	0.9998	0.9896	0.9966	0.0043
45/35 °C	0.9993	0.9856	0.9968	0.0046
35/25 °C	0.9903	0.9890	0.9895	3.512e-04

In Part 2, the calculated wall temperature distributions were compared to the default ones. The MAPDs of the calculated wall temperature distributions with respect to the default ones is shown below in Table 7. Note that the standard deviation is given in percentage points.

Table 7. Results for validation of Case A, Part 2

Temperature set	Maximum (%)	Minimum (%)	Mean (%)	Standard deviation (%)
55/45 °C	1.719e-04	4.586e-05	9.860e-05	3.274e-05
45/35 °C	2.065e-04	1.055e-05	6.552e-05	6.686e-05
35/25 °C	5.979e-04	2.022e-04	3.304e-04	1.081e-04

Finally, in Part 3, the average Nusselt value calculated was compared to that calculated using the reference study. The results are presented in Table 8 below. Note that here, as well, the standard deviation is given in percentage points.

Table 8. Results for validation of Case A, Part 3

Temperature set	Maximum (%)	Minimum (%)	Mean (%)	Standard deviation (%)
55/45 °C	5.599	1.730	2.996	1.034
45/35 °C	5.623	1.843	3.026	1.028
35/25 °C	5.706	1.899	3.105	1.035

3.3.2 Validation results for Case B

For Case B, the case with potentially various convection types, the result from Part 1 of the validation – the linear approximation of the region with forced and/or mixed convection – are presented in Table 9 below.

Table 9. Results for validation of Case B, Part 1

Temperature set	Maximum R ²	Minimum R ²	Mean of R ²	Standard deviation of R ²
55/45 °C	0.9984	0.9919	0.9958	9.5486e-04
45/35 °C	0.9993	0.9927	0.9985	7.451e-04
35/25 °C	0.9993	0.9211	0.9748	0.0158

Next, in Part 2, still treating the region with forced/mixed convection, the average Nusselt values calculated can be compared to those from calculations based on the reference study and the MAPDs are found. The results are presented in Table 10 below.

Table 10. Results for validation of Case B, Part 2

Temperature set	Maximum (%)	Minimum (%)	Mean (%)	Standard deviation (%)
55/45 °C	181.3	133.4	157.8	9.630
45/35 °C	165.9	116.7	139.7	9.587
35/25 °C	12 300	83.49	123.5	260.9

Similarly, such results are presented for the part with natural convection, for the cases where such a part indeed exists. This constitutes Part 3 and 4 of the validation and correspond to Part 1 and 3 of the Case A validation. The results are seen in Table 11 and 12 below.

Table 11. Results for validation of Case B, Part 3

Temperature set	Maximum R^2	Minimum R^2	Mean of R^2	Standard deviation of R^2
55/45 °C	0.9999	0.2974	0.9691	0.1086
45/35 °C	0.9995	0.0463	0.9675	0.1104
35/25 °C	0.9984	0.3735	0.9742	0.1076

Table 12. Results for validation of Case B, Part 4

Temperature set	Maximum (%)	Minimum (%)	Mean (%)	Standard deviation (%)
55/45 °C	1270	0.6502	46.61	143.5
45/35 °C	1933	2.361	58.63	190.4
35/25 °C	875.3	2.461	42.94	106.6

3.3.3 Final validation overview

The difference between calculated and literature values are presented in Figure 14 below. Here MAPD between calculated and literature Nusselt values is shown for every respective case calculated. As should be noted, there is a large deviation between calculated and literature values for Case B. The comparative success of validation of Part A is seen clearly, which constitutes the bound of $u_\infty=0$ of the surface, along the height axis. All results are further discussed below.

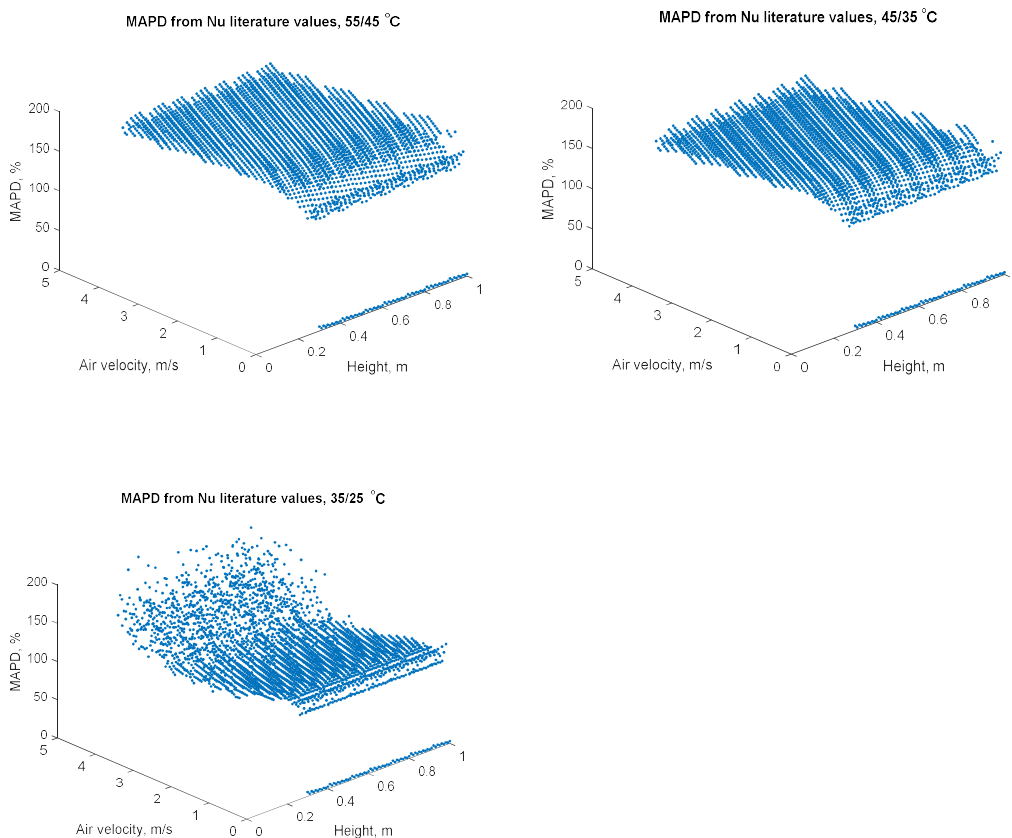


Figure 14. MAPD between calculated and literature Nusselt values

3.4 Additional results concerning the 2002 reference study

As is seen by the results, there turns out to be a large deviation between values calculated by the model used in this thesis and those values calculated based on the 2002 reference study (Gavara et al, 2012). This is evident by Table 12 above.

Much like for the investigation done in this thesis, the 2002 reference study uses few reference studies (Gavara et al, 2012). For the isothermal case, the reference study is validated. However, further validation for the reference study was not possible due to the lack of experimental studies of the non-isothermal case. Below, a simple example is used to demonstrate the large difference between values from the two methods of calculation.

Intuitively, the convective heat output from a linear temperature profile should be somewhere between the heat outputs for constant temperature profiles (i.e. isothermal plates) of the maximum and minimum temperatures of the linear distribution. The convective heat output is proportional to the convective heat transfer coefficient, which in turn is proportional to the Nusselt value. Consequently, the Nusselt value for the linear temperature profile could with this reasoning be expected to be somewhere between those for isothermal configurations of the two respective extreme temperatures. For example, for the case of the temperatures 45/35, the expected relationship would then be either:

$$Nu_{av,iso,35} < Nu_{av,45/35} < Nu_{av,iso,45}, \text{ or:}$$

$$Nu_{av,iso,45} < Nu_{av,45/35} < Nu_{av,iso,35}$$

In the proceeding part, calculations are performed based on the reference study for the three cases above – isothermal plate at 35 °C, plate with linear temperature profile, ranging from 35 to 45 °C, and isothermal plate at 45 °C. This is meant to compare results derived from the reference study.

The simplified method used here is based on a height $H = 500$ mm. Ten cells are considered, $n = 10$. The freestream velocity is taken to be $u = 2.0$ m/s. Constants are used similar to earlier calculations, and relevant air properties are taken to be constant, such that $\nu = 1.5 \times 10^{-5}$ m²/s and $\beta = 3.4 \times 10^{-3}$ 1/K.

Calculations for the three different cases are presented in Table 13 through 16 below. Note that values are rounded off.

Table 13. Key results for isothermal vertical flat plate at 35 °C

Isothermal vertical flat plate at 35 °C											
Cell	y_{mid} (mm)	T_w (K)	λ_0	λ_1	$(\lambda_0)^2$	$Re^{1/2}$	Gr	Ri	$H'(0)$	Nu	
1	25	35	0	0	0	3333	34744	2.81E-10	-0.2942	9.81E+02	
2	75	35	0	0	0	10000	938081	9.4E-11	-0.2942	2.94E+03	
3	125	35	0	0	0	16667	4342969	5.6E-11	-0.2942	4.90E+03	
4	175	35	0	0	0	23333	11917106	4E-11	-0.2942	6.87E+03	
5	225	35	0	0	0	30000	25328194	3.1E-11	-0.2942	8.83E+03	
6	275	35	0	0	0	36667	46243931	2.6E-11	-0.2942	1.08E+04	
7	325	35	0	0	0	43333	76332019	2.2E-11	-0.2942	1.27E+04	
8	375	35	0	0	0	50000	1.17E+08	1.9E-11	-0.2942	1.47E+04	
9	425	35	0	0	0	56667	1.71E+08	1.7E-11	-0.2942	1.67E+04	Nu_{av}
10	475	35	0	0	0	63333	2.38E+08	1.5E-11	-0.2942	1.86E+04	9807

Table 14. Key results for isothermal vertical flat plate at 45 °C

Isothermal vertical flat plate at 45 °C											
Cell	y_{mid} (mm)	T_w (K)	λ_0	λ_1	$(\lambda_0)^2$	$Re^{1/2}$	Gr	Ri	$H'(0)$	Nu	
1	25	45	0	0	0	3333	57906	4.69E-10	-0.2942	9.81E+02	
2	75	45	0	0	0	10000	1563469	1.56E-10	-0.2942	2.94E+03	
3	125	45	0	0	0	16667	7238281	9.4E-11	-0.2942	4.90E+03	
4	175	45	0	0	0	23333	19861844	6.7E-11	-0.2942	6.87E+03	
5	225	45	0	0	0	30000	42213656	5.2E-11	-0.2942	8.83E+03	
6	275	45	0	0	0	36667	77073219	4.3E-11	-0.2942	1.08E+04	
7	325	45	0	0	0	43333	1.27E+08	3.6E-11	-0.2942	1.27E+04	
8	375	45	0	0	0	50000	1.95E+08	3.1E-11	-0.2942	1.47E+04	
9	425	45	0	0	0	56667	2.84E+08	2.8E-11	-0.2942	1.67E+04	Nu_{av}
10	475	45	0	0	0	63333	3.97E+08	2.5E-11	-0.2942	1.86E+04	9807

Table 15. Key results for vertical flat plate with linearly dropping temperature profile, 45/35 °C (1)

Vertical flat plate with linearly dropping temperature profile, 45/35 °C (1)								
Cell	y_{mid} (mm)	T_w (K)	λ_0	λ_1	$(\lambda_0)^2$	$Re^{1/2}$	Gr	Ri
1	25	35.5	0.033	0	0	3334	57907	4.7E-10
2	75	36.5	0.091	0	0	10000	1563469	1.57E-10
3	125	37.5	0.143	0	0	16667	7238282	9.4E-11
4	175	38.5	0.190	0	0	23334	19861844	6.8E-11
5	225	39.5	0.231	0	0	30000	42213657	5.3E-11
6	275	40.5	0.269	0	0	36667	77073219	4.3E-11
7	325	41.5	0.303	0	0	43334	1.27E+08	3.7E-11
8	375	42.5	0.334	0	0	50000	1.95E+08	3.2E-11
9	425	43.5	0.362	0	0	56667	2.84E+08	2.8E-11
10	475	44.5	0.388	0	0	63334	3.97E+08	2.5E-11

Table 16. Key results for vertical flat plate with linearly dropping temperature profile, 45/35 °C (2)

Vertical flat plate with linearly dropping temperature profile, 45/35 °C (2)							
Cell	$H'(0)$	T_w (K)	θ'_0	θ'_1	θ'_{00}	Nu	
1	-0.2942	35.5	-0.1871	0.0416	8.45E-12	1.00E+03	
2	-0.2942	36.5	-0.1871	0.0416	3.00E-12	3.11E+03	
3	-0.2942	37.5	-0.1871	0.0416	1.91E-12	5.35E+03	
4	-0.2942	38.5	-0.1871	0.0416	1.44E-12	7.69E+03	
5	-0.2942	39.5	-0.1871	0.0416	1.18E-12	1.01E+04	
6	-0.2942	40.5	-0.1871	0.0416	1.02E-12	1.26E+04	
7	-0.2942	41.5	-0.1871	0.0416	9.01E-13	1.52E+04	
8	-0.2942	42.5	-0.1871	0.0416	8.17E-13	1.78E+04	
9	-0.2942	43.5	-0.1871	0.0416	7.53E-13	2.05E+04	
10	-0.2942	44.5	-0.1871	0.0416	7.03E-13	2.32E+04	
						Nu_{av}	1.17E+04

As can be seen with the cases presented above, the isothermal cases obtain very similar Nusselt values. The linear case, however, obtains a rather different Nusselt value, some 19 % larger. This has interesting consequences for the discussion of the validity of the reference study and thermal engineering in general, as is further discussed above.

4 Discussion

4.1 Final results

The calculated values can be fit with the polynomials presented with very good accuracy. Still, some results yielded by using the polynomial relationships found can contain large errors. This is especially true at the edges of the domain for which the approximation has been created. However, overall, the polynomial fits are considered largely accurate.

It should be noted that the heat flux remains almost unchanged with the radiator height. This is due to the study model being used, in which the radiator water flow, and hence the temperature drop along it, is set to be the same for all heights at zero freestream air velocity. Consequently, the difference of heat flux for the different radiator heights become very small as long as the freestream air velocity is zero. Larger heat flux differences can clearly be seen between radiator heights as the freestream velocity is increased, showing the advantage of low-height radiators in this regard.

The differences between the three temperature set-ups largely correspond to what could be expected. Decreasing the radiator temperature set-up basically means a parallel shift of the curve towards lower heat transfer, be it in terms of total heat transfer or heat flux. Some features are somewhat different, such as the increment of heat transfer as the freestream velocity is increased. Regardless of this, the overall shape of the surfaces (seen in Figure 12 and 13 above) used to present the polynomial approximation basically remains unchanged with changing temperature set-ups.

4.2 Calculation method

Some comments should be made on the calculation method used. For certain inputs, the convergence process has not been working as desired, and thus a few extreme outlier points occur among the data points. Properly controlling the efficacy and validity of the iterative calculation algorithm used in this investigation would require more work, and this falls outside of the scope of what this investigation has been meant to accomplish. More thorough testing and modification could be made for calculation convergence. Thus, it could be ensured that proper convergence always occur, regardless of initial conditions set-up to start calculations. This becomes in itself an important activity, ensuring the uniqueness of temperature profile that a wall would converge towards in a steady state. If there was – in fact – no uniqueness, another aspect of optimization could possibly be finding starting conditions yielding the most desired steady state result.

4.3 Validation

As a consequence of the calculation method used, some outliers exist among the yielded data points. This is important to note before discussing the validation results in greater detail. However, only a few data points yielded become clearly anomalous, and this has only small effect on the study outcome.

Overall, the study can be said to be fully validated for Case A – where natural convection is studied – but only to a very limited extent, if at all, for the mixed regimes of convection of Case B. In the following, some comments will be made on the individual parts of the validation.

For Case A, the validation is generally successful. In Part 1 a very clear linearity is seen. This linearity is also shown in Part 2. Next, Part 3 shows that the results have a very small difference with those of the 1999 reference study (more precisely: Havet & Blay, 1999), thus validating the results found for Case A.

For Case B, however, the validation is nowhere near as successful. Part 1 shows overall a clear linearity of the calculated wall temperature profile. For lower temperatures, this is less clear.

However, this deviation could possibly largely be a result of problems with the calculation method used.

In Part 2 of Case B large deviations between the calculated values and the reference study are seen. Some of the extreme results might be explained by the calculation method used. However, the fact remains that the results differ greatly. Perhaps all this is due to a lacking understanding of the study, and an incorrect use of study results. This is discussed further in 4.4 below.

Part 3 for Case B is overall acceptable. Some extreme values occur, but there is overall reasonable linearity. Poorer results are obtained here than for the natural convection of Case A Part 1. This could largely be due to the few points constituting regions of natural convection in Case B. Throughout the work with this investigation, linearity has been found to be poorer for regions with fewer points, partly because of an increased sensibility to more extreme outliers.

As for Part 4, the results are also acceptable, considering there is not a full linearity (as seen in Part 3), and that the reference study is used somewhat outside its designated area (as the freestream velocity is not zero). In conclusion, Part 3 and 4 are thus considered reasonably successful at validating calculated values.

4.4 Further comments

To continue, further comments should be made on the 2012 reference study (Gavara et al, 2012). There could be various reasons for the large deviation of results. Up to this point, only potential shortcomings of this investigation have been presented. Another option, however, is that the results of the 2012 study are incorrect. In Appendix B, an argument is made about approximate results that possibly are to be expected. However, with the example calculated, some interesting results are found. It is there seen that, according to the 2012 study, the Nusselt number can be significantly increased along a wall if it is subject to linear wall temperature profile rather than an isothermal configuration. This could indicate potential problems with the study, which has been shown to yield Nusselt values considerably higher than those calculated.

Further comments can be made on the interesting results from the reference study. If these are, indeed, correctly calculated based on the reference study, this potentially opens for many possibilities in thermal engineering. For example, it presents an analytical approach to heat transfer optimization problems, where current approaches often resolve around numerical simulation. As with many other heat transfer related issues, there is a very large area of applications. Judging by results obtained using the reference study, a large part of the optimization would consist of obtaining an appropriate wall temperature distribution to – depending on application – maximize or minimize heat transfer. Wall temperature distribution could be modified by how heat is lead to such a wall. Also it could be made up of different materials with varying thickness, changing Bi number and other properties along the wall.

However, what has become clear during the finalization of this investigation is the need for further experimental studies on varying wall temperature configurations for the case of the flat vertical heated wall. Only few studies have been found that treat other cases than that which is isothermal.

To finally relate the results of the investigation to HVAC applications, the results clearly show the benefit of low-height forced convection systems, such as baseboard radiators. Such systems clearly have the potential of heating efficiently relative to system area and material needed.

5 Conclusion

It is concluded that accurate values are calculated for Case A, the case with natural convection. For Case B, values are found to differ greatly with values of the reference study used. Potential reasons for this difference are discussed. Besides of the issue of validation for Case B, the method used in this investigation produces fairly reliable values. It is thus seen that nothing can be firmly concluded with regard to heat transfer of a linear wall temperature profile in a regime of mixed or forced convection. This investigation produces an estimate to what such values might be, but there is a clear need of further experimental studies in this area.

6 Future Work

There is at the present time only scant literature on heat transfer from flat vertical plates with non-isothermal temperature profiles. For a greater understanding of this area, more experimental work seems to be needed.

The 2012 reference study (Gavara et al, 2012) presents a very interesting approach to the problem, and possibly solves it for an arbitrary wall temperature distribution. This promising approach can be used for a range of optimization problems, e g heat exchanger optimization, offering a more analytical approach to an area where numerical solution is common.

As for this investigation, possible expansion includes a more thorough validation of the calculation method used and an expansion of cases considered. For example, more cases for T_{sup} and T_{ret} could be considered, and other values for ΔT . Thus, it could more clearly be seen how these parameters relate to heat transfer. Also, the case of a non-steady state of a vertical flat plate non-isothermal heat transfer system could be further investigated. Finally, more can be investigated in terms of different wall temperature profiles and the case of constant capacity rate systems.

7 References

- Boerstra, A., Veld, P. O., Eijdens, H. 2000. *The Health, Safety and Comfort Advantages of Low Temperature Heating Systems: A Literature Review*. Proceedings of the 6th International Conference on Healthy Buildings.
- Boverkets byggregler (föreskrifter och allmänna råd), BBR BFS 2011:6 med ändringar till och med BFS 2017:5*. 2017. [Updated version of Swedish Building Code]. BFS 2011:6 with changes up to and including BFS 2017:5. Access: <https://www.boverket.se/sv/lag--ratt/forfattningssamling/gallande/bbr---bfs-20116/> [2017-10-15].
- Boverkets föreskrifter om ändring i verkets byggregler (2011:6) - föreskrifter och allmänna råd*. 2015. [Changes in Swedish Building Code]. Stockholm. BFS 2015:3.
- Calisir, T., Baskaya, S., Yazar, H. O., Yucedag, S. 2015. *Experimental investigation of panel radiator heat output enhancement for thermal use under actual operating conditions*. Access: http://epjwoc.epj.org/articles/epjconf/pdf/2015/11/epjconf_efm2014_02010.pdf [2017-10-15].
- Churchill, S. W. & Chu, H. H. S. 1975. *Correlating equations for laminar and turbulent free convection from a vertical plate*. IJHMT, 18 (1975), pp. 1323-1329. Access: <http://www.sciencedirect.com/science/article/pii/0017931075902434> [2017-10-15].
- Dodge Data & Analytics. 2016. *World Green Building Trends*. Access: <http://fidic.org/sites/default/files/World%20Green%20Building%20Trends%202016%20SmartMarket%20Report%20FINAL.pdf> [2017-10-05].
- elementflakten.se. 2016. [Webpage]. Access: <http://www.elementflakten.se/> [2017-10-15].
- European Commission. 2010. *EUROPE 2020 – A strategy for smart, sustainable and inclusive growth*. Access: <http://ec.europa.eu/eu2020/pdf/COMPLET%20EN%20BARROSO%20%20%20007%20-%20Europe%202020%20-%20EN%20version.pdf> [2017-10-15].
- Fanger, P. O., 1970. *Thermal comfort analysis and applications in environmental engineering*. New York: McGraw-Hill.
- Fastighetvärlden. 2015. *Miljardsatsning på rustning av miljonprogrammet*. Access: <http://www.fastighetsvarlden.se/notiser/miljardsatsning-pa-rustning-av-miljonprogrammet/> [2017-10-15].
- Gavara, M. R., Dutta, P., Seetharamu, K. N. 2012. *Mixed convection adjacent to non-isothermal vertical surfaces*. IJHMT, 55 (2012), pp. 4580-4587. Access: <http://www.sciencedirect.com/science/article/pii/S0017931012002451> [2017-10-15].
- Grundfos. 2017. [Webpage]. Access: <http://www.grundfos.com/service/encyclopedia-search/two-pipe-system.html> [2017-08-04].
- Havet, M. & Blay, D. 1999. *Natural convection over a non-isothermal vertical plate*. IJHMT, 42 (1999), pp. 3103-3112. Access: <http://www.sciencedirect.com/science/article/pii/S0017931098003743> [2017-10-15].
- Holman, J. P. 2010. *Heat Transfer*. 10th edition. New York: McGraw-Hill.
- Johansson, P-O. 2011. *BUILDINGS AND DISTRICT HEATING – contributions to development and assessment of efficient technology*. Diss. Lund University. Lund: E-husets Tryckeri.

- Jonsson, P. & Ahlstrand, J. 2005. *Forced convection in low temperature heating systems*. Bachelor's thesis. KTH Royal Institute of Technology. Stockholm.
- McQuillan, F. J., Culham, J. R., Yovanovich, M. M. 1984. *Properties of dry air at one atmosphere*. Access: http://www.mhtlab.uwaterloo.ca/pdf_reports/mhtl_G01.pdf [2017-08-04].
- Ploskić, A. 2010. *Low-Temperature Baseboard Heaters in Built Environments*. Lic. KTH Royal Institute of Technology. Stockholm.
Access: <http://kth.diva-portal.org/smash/get/diva2:359656/FULLTEXT01.pdf> [2017-08-04].
- radiatoren.blogspot.se. 2017. *Types van radiatoren: Welke types zijn er en wat is het verschil*. [“Radiator types: What types are there and how do they differ”]. Access: <http://radiatoren.blogspot.se/p/type-radiatoren.html#.WXdQuljyi00> [2017-10-15].
- RADSON. 2016. *The guide to radiators for low temperature heating*. [Webpage]. Access: http://www.radson.com/docs/HeatingGuide_OT_LR.pdf [2016-07-20].
- Seppänen, O., Fisk, W. J., Lei, Q. H. 2005. *Ventilation and performance in office work*. International Journal of Indoor Environment and Health, 16 (2006), pp. 28-36.
- SS EN 442. 1996. *Radiators and convectors*. European standard.
- Statens energimyndighet. 2015. [Swedish Energy Agency]. *Energiläget 2015*. Access: https://www.energimyndigheten.se/contentassets/50a0c7046ce54aa88e0151796950ba0a/energilaget-2015_webb.pdf [2017-08-04].
- Trüschel, A. 1999. *Värmesystem med luftvärmare och radiatorer. En analys av funktion och prestanda*. Lic. Chalmers, Gothenburg.
- van der Wijst, R. P. M. M. 2010. *Improved performance of hydronic heating systems connected to district heating*. Access: http://www.ees.energy.lth.se/fileadmin/ees/Publikationer/2011/Roy_LTH_report.pdf [2017-10-15].
- Wang, Q. & Holmberg, S. 2015. *Combined Retrofitting with Low Temperature Heating and Ventilation Energy Savings*. 6th International Building Physics Conference, IBPC 2015. Energy Procedia 78 (2015) pp. 1081 – 1086.
- Warfvinge, C. & Dahlbom, M. 2010. *Projektering av VVS-installationer*. Lund: Studentlitteratur.
- Wylie, R. G. 1973. *The transfer coefficients of a laminar boundary layer with variable fluid properties*. Chem. Engineering, 6 (1973), pp. 1-4. Access: <http://www.sciencedirect.com/science/article/pii/0300946773850166> [2017-08-04].

Appendix A

A.1 Main code

```
% RADIATOR HEAT TRANSFER
% Version 1.8, 2016-10-23
% Written by: Oskar Scheibe
%
% Description: This program calculates the heat output from a simplified
% radiator model. Calculations are based on empirical equations for a
% vertical flat plate. Both radiation and convection are taken into
% account.
%
% The vertical flat plate is heated with a heat capacity rate (denoted C),
% i e mass flow x specific heat capacity. This flow is set to be constant
% for every height H. For the base case of freestream velocity u = 0, C is
% set so that the temperature drop over the height, dT, is 10 K.
%
% The temperature profile and heat output for every configuration of height
% (H) and freestream velocity (u) are found through iterative calculations.
% The cases for full natural convection (u = 0) and those with non-zero
% freestream velocity are separately compared to calculated values based
% on reference studies, to test the validity of obtained results.
%
% Program overview:
% - Initial set-up
% - Heat transfer for u = 0
% - Validation of results, zero freestream velocity
% - Heat transfer for u > 0
% - Validation of results, non-zero freestream velocity
% - - - - -

% INITIAL SET-UP:

% Values for height, H:
H_lower_bound = 0.30;
H_upper_bound = 1.00;
H_step_size = 0.01;
points_H = round((H_upper_bound-H_lower_bound)/H_step_size+1);

% Values for non-zero freestream velocity, u:
u_lower_bound = 0.1;
u_upper_bound = 5.0;
u_step_size = 0.1;
points_u = round((u_upper_bound-u_lower_bound)/u_step_size+2);

% Empty lists to store results:
results_linear_approx_MC_part = zeros(points_u-1,points_H);
results_linear_approx_NC_part = zeros(points_u-1,points_H);
results_MAPD_Nu_MC_part = zeros(points_u-1,points_H);
results_MAPD_Nu_NC_part = zeros(points_u-1,points_H);
results_NC_linear_approx_MAPD = zeros(1,points_H);
results_NC_linear_approx_R_sqr = zeros(1,points_H);
results_NC_Nu_MAPD = zeros(1,points_H);
results_point_shift = zeros(points_u-1,points_H);
results_total_heat_transfer = zeros(points_u,points_H);
```

```

% Value for width, w:
w = 1; % w = 1 is used for the sake of simplicity.
      % Value chosen is arbitrary.

% Freestream temperature:
T_inf = 273 + 20; % Could also be regarded as average room temperature.

% Some physical constants:
g = 9.81; % Gravitational acceleration.
epsilon_rad = 0.9; % Radiator emissivity.
sigma = 5.67e-8; % Stefan-Boltzmann constant.

for H = H_lower_bound:H_step_size:H_upper_bound;
    % CONTINUED SET-UP:

    % Number of H for which calculations are made:
    number_H = round((H-H_lower_bound)/H_step_size+1);

    % Number of cells, n:
    n = round(H/1e-3); % Number of cells along radiator height, 1 per 1 mm.

    % Supply and return temperatures:
    T_sup = 273 + 35; % Radiator supply temperature.
    T_ret = 273 + 25; % Radiator return temperature.

    % Initial temperature distribution:
    T_w = T_ret:(T_sup-T_ret)/n:T_sup; % Linear distribution.

    % Temperature drop over radiator:
    dT = T_sup - T_ret;

    % Starting value for heat capacity rate, C, for base case:
    C = 0; % Arbitrary, later adjusted.

    % Nonzero velocity:
    u = 0; % Initial velocity supplied by fan. Note: u >= 0.

    % Max relative difference between single cell temperatures between
    % iterations:
    max_change = 1; % Arbitrary starting value.

    % Starting value for number of cell of first shift to natural from
    % other convection mode. Set outside range:
    point_shift = n+1;

    % Cell area:
    A_cell = w*H/n;

    % Lists of positions along the height:
    y_upper_bound = H/n:H/n:H; % Heights corresponding to
                                % temperature points of T_w, except
                                % for the first one.

    y_mid = H/(2*n):H/n:(2*n-1)*H/(2*n); % Midpoints for cells.

    % FULL NATURAL CONVECTION:

    while max_change > 1e-2;

```

```

% Calculating relevant temperatures:
[ LMTD_cell, LMTD_acc, T_f_local_av, T_f_acc_av ] = ...
    WallTemperaturesCalc( T_w, T_inf );
% Calculating relevant air properties:
[ lambda, beta, ny, alpha] = AirProperties( T_f_local_av, ...
    T_f_acc_av );
% Calculating dimensionless numbers along the plate:
[ Pr, Gr, Ra, Re, Ri ] = DimlessNumbers( ny, alpha, g, beta, ...
    LMTD_acc, y_upper_bound, u );
% Calculating radiative heat output:
[ Q_rad ] = RadiativeHeatOutput( T_w, T_inf, epsilon_rad, ...
    sigma, A_cell, LMTD_cell );
% Calculating convective heat output:
[ Nu_total_av, Nu_local_av, Q_con ] = ...
    ConvectiveHeatOutput( n, Ra, Pr, Re, Ri, y_upper_bound, ...
    lambda, y_mid, A_cell, LMTD_cell );
% Updating temperature profile:
[ Q_tot, T_w, max_change, T_ret, dT, C ] = ...
    CalcValuesUpdate( T_w, T_sup, T_ret, T_inf, C, Q_rad, ...
    Q_con, n, 0 );
end

% VALIDATION FOR FULL NATURAL CONVECTION:

% (1) Testing linearity of temperature profile T_w:
[ R_sqr_MLS, T_w_MLS_best_fit ] = TestLinearity( T_w, H, ...
    point_shift, n, 0 );
% CalcMode at 0.

% (2) Finding mean absolute percentage deviation (MAPD):
[ MAPD_NC ] = TestMAPDNC( T_w, T_sup, T_ret, n );

% (3) Comparing Nu-values:
[ MAPD_Nu ] = TestNuNC( T_w, n, point_shift, H, T_inf, g, ...
    Nu_local_av, 0 );
% CalcMode at 0.

% Saving values for natural convection:
results_total_heat_transfer(1,number_H) = sum(Q_tot);
results_NC_linear_approx_MAPD(number_H) = MAPD_NC;
results_NC_linear_approx_R_sqr(number_H) = R_sqr_MLS;
results_NC_Nu_MAPD(number_H) = MAPD_Nu;

% CONVECTION OF VARIED FORM:
for u = u_lower_bound:u_step_size:u_upper_bound;

    % The number of the value of u:
    number_u = round((u-u_lower_bound)/u_step_size+1);

    % Resetting parameter for convergence
    max_change = 1;

while max_change > 1e-2;
    % Calculating relevant temperatures:
    [ LMTD_cell, LMTD_acc, T_f_local_av, T_f_acc_av ] = ...
        WallTemperaturesCalc( T_w, T_inf );
    % Calculating relevant air properties:
    [ lambda, beta, ny, alpha] = AirProperties( T_f_local_av, ...
        T_f_acc_av );
    % Calculating dimensionless numbers along the plate:
    [ Pr, Gr, Ra, Re, Ri ] = DimlessNumbers( ny, alpha, g, beta, ...
        LMTD_acc, y_upper_bound, u );

```

```

% Calculating radiative heat output:
[ Q_rad ] = RadiativeHeatOutput( T_w, T_inf, epsilon_rad, ...
    sigma, A_cell, LMTD_cell );
% Calculating convective heat output:
[ Nu_total_av, Nu_local_av, Q_con ] = ...
    ConvectiveHeatOutput( n, Ra, Pr, Re, Ri, y_upper_bound, ...
    lambda, y_mid, A_cell, LMTD_cell );
% Updating temperature profile:
[ Q_tot, T_w, max_change, T_ret, dT, C ] = ...
    CalcValuesUpdate( T_w, T_sup, T_ret, T_inf, C, Q_rad, ...
    Q_con, n, 1 );
end

% VALIDATION FOR CONVECTION OF VARIED FORM:

% Finding point where there is shift between Forced/Mixed Convection
% and Natural Convection:
[ point_shift ] = FindPointShift( Ri, n );

% Validation of non-natural convection part:

% (1) Testing linearity of relevant part of temperature profile T_w:
[ R_sqr_MLS, T_w_MLS_best_fit ] = TestLinearity( T_w, H, ...
point_shift, n, 0 ); % CalcMode at 0.

% (2) Comparing Nu-values:
[ MAPD_Nu_nonNC ] = TestNunonNC( T_w_MLS_best_fit, T_inf, ...
    y_mid, Ri, u, n, H, point_shift, Nu_local_av );

% Saving results:
results_linear_approx_MC_part(number_u,number_H) = R_sqr_MLS;
results_MAPD_Nu_MC_part(number_u,number_H) = MAPD_Nu_nonNC;

% Validation of natural convection part (when there is any):

% (1) Testing linearity of relevant part of temperature profile T_w:
[ R_sqr_MLS, T_w_MLS_best_fit ] = TestLinearity( T_w, H, ...
    point_shift, n, 1 ); % CalcMode at 1.

% (2) Comparing Nu-values:
[ MAPD_Nu ] = TestNuNC( T_w, n, point_shift, H, T_inf, g, ...
    Nu_local_av, 1 ); % CalcMode set to 1.

% Saving results:
results_linear_approx_NC_part(number_u,number_H) = R_sqr_MLS;
results_MAPD_Nu_NC_part(number_u,number_H) = MAPD_Nu;
results_total_heat_transfer(number_u+1,number_H) = sum(Q_tot);
results_point_shift(number_u,number_H) = point_shift;

end

end

```

A.2 Functions

Function WallTemperaturesCalc

```
function [ LMTD_cell, LMTD_acc, T_f_local_av, T_f_acc_av ] = ...
    WallTemperaturesCalc( T_w, T_inf )
% WallTemperaturesCalc: Given a specific wall temperature distribution, the
% function returns the temperature values needed for calculations.
%
% LMTD_cell: LMTD over a single calculation cell. Used for calculating
% cell heat output.
%
% LMTD_acc: Accumulated LMTD from bottom up to certain point along wall
% height. Used for calculating heat output from an area with certain
% height.
%
% T_f_local_av: Average film temperature for cell. Used for evaluating
% cell's average lambda value.
%
% T_f_acc_av: Average film temperature for wall area up to certain
% height. Used for evaluating various air properties.

LMTD_cell = diff(T_w)./log((T_w(2:end)-T_inf)./(T_w(1:(end-1))-T_inf));

LMTD_acc = (T_w(2:end)-T_w(1))./log((T_w(2:end)-T_inf)/(T_w(1)-T_inf));

T_f_local_av = ((T_w(2:end)+T_w(1:(end-1)))/2+T_inf)/2;

% Creating empty list for T_f_acc_av:
T_f_acc_av = zeros(1,length(T_w)-1);

% Defining T_f_acc_av:
for i = 1:length(T_w)-1;
    T_f_acc_av(i) = (sum(T_w(1:i+1))/i+T_inf)/2;
end

end
```

Function TestNunonNC

```
function [ MAPD_Nu_nonNC ] = TestNunonNC( T_w_MLS_best_fit, T_inf, ...
    y_mid, Ri, u, n, H, point_shift, Nu_local_av )
% TestNunonNC: Given a best-fit linear wall temperature distribution, this
% function calculates an average Nusselt value by using a method from
% literature (see thesis for further description). It finally compares the
% Nusselt value obtained from iterative calculation with corresponding
% value obtained from the method described in literature.
%
% MAPD_Nu_nonNC: Mean absolute percentage deviation between average
% Nusselt value calculated by iterative method and by method described in
% literature.

% Some constant properties are needed for calculations based on literature
% method. These are calculated below.
```

```

% Calculating average film temperature:
T_f_av = (sum(T_w_MLS_best_fit)/length(T_w_MLS_best_fit)+T_inf)/2;

% Calculating ny:
ny = 1/(2.4090e8/T_f_av^(3/2)+2.6737e10/T_f_av^(5/2));

% Calculating Re:
Re = [u*y_mid(1:point_shift-1)/ny]';

% Some pre-defined coefficient values from literature (Gavara et al, 2012)
% are needed. These are function values for when parameter eta is equal to
% zero.

% Corresponding values of Ri:
Ri_coefficients = [0.0 0.01 0.04 0.1 0.4 1.0 2.0 4.0 10.0]';

% Coefficient values:
H_prime = [-0.2942 -0.2965 -0.3029 -0.3151 -0.3548 -0.4040 -0.4563 ...
            -0.5233 -0.6377]';
theta_zero_prime = [-0.1871 -0.1888 -0.1936 -0.2014 -0.2341 -0.2743 ...
                    -0.3162 -0.3686 -0.4551]';
theta_one_prime = [0.0416 0.042 0.0431 0.0446 0.0519 0.0608 ...
                   0.0701 0.0817 0.1008]';
theta_zerozero_prime = [0 0.0003 0.0012 0.0024 0.0057 0.0086 ...
                        0.0109 0.0135 0.0212]';

% These can be organized into a matrix such that:
coefficient_matrix = [H_prime,theta_zero_prime,theta_one_prime,...
                     theta_zerozero_prime];

% For all cells with non-natural convection, coefficient values are
% calculated using cubic spline interpolation.

% Empty matrix to store values:
values_coefficients = ones(point_shift-1,4);

for i = 1:point_shift-1;    % For cells with non-natural convection
    % Local value for Ri:
    Ri_cell = Ri(i);

    % Calculating value by interpolation:
    for k = 1:4;           % Matrix has 4 columns.
        function_values = coefficient_matrix(:,k);
        value_interpolated = spline(Ri_coefficients, function_values, ...
                                    Ri_cell);
        % Saving value:
        values_coefficients(i,k) = value_interpolated;
    end
end

% Calculating lambdas according to study (Gavara et al, 2012). A linear
% function is used to best fit the data. The function has form  $y = mx + c$ ,
% with  $m = T_{sup} - T_{ret}$  and  $c = T_{ret} - T_{inf}$ . It can be seen that
% lambda_one is equal to zero, as the second derivative of y is zero.

% Calculating m:
m = (T_w_MLS_best_fit(point_shift)-T_w_MLS_best_fit(1))/...

```

```

        ((point_shift-1)/n*H);

% Calculating c:
c = T_w_MLS_best_fit(1)-T_inf;

% Calculating lambda_zero:
lambda_zero = [m*y_mid(1:point_shift-1)./(m*y_mid(1:point_shift-1)+c)]';

% Finding Nusselt value:
Nu = (Re.^(1/2)).*-(values_coefficients(:,1)+lambda_zero.*...
    values_coefficients(:,2)+lambda_zero.^2.*values_coefficients(:,4));

% Mean absolute percentage deviation:
MAPD_Nu_nonNC = sum(abs((Nu-Nu_local_av(1:point_shift-1)') ./...
    Nu*100))/length(Nu);

end

```

Function TestNuNC

```

function [ MAPD_Nu ] = TestNuNC( T_w, n, point_shift, H, T_inf, g, ...
    Nu_local_av, CalcMode )
% TestNuNC: Given a linear wall temperature profile, this function
% calculates an average Nusselt value using relationships described in a
% literature study ((Havet & Blay, 1999), for explanation, see thesis
% text). Following this, a comparison is made between the obtained value
% and that which has earlier been calculated iteratively.
%
% S: Slope of original T_w. S = dT_w/dy. Note: Units are K/cm.
%
% MAPD_Nu: Mean absolute percentage deviation between average Nusselt
% value calculated by iterative method and by method described in
% literature.
%
% CalcMode: Variable determining which part of the plate is calculated.
% If CalcMode = 0, calculations are made for the entire plate (the case
% of full natural convection).
% If CalcMode = 1, the entire plate does not have natural convection.
% Calculation are thus only made for the relevant region of the plate.

% Determining relevant temperatures for the calculations:

% Upper temperature:
T_upper = T_w(n+1);

% Lower temperature:
if point_shift ~= n+1;
    T_lower = T_w(point_shift);
else
    T_lower = T_w(1);
end

% Determining relevant Nusselt values for the calculations:
if CalcMode == 0;
    Nu_av = sum(Nu_local_av)/n;
else

```



```

if point_shift ~= n+1;
    Nu_av = sum(Nu_local_av(point_shift:n))/(n-point_shift);
else
    Nu_av = -1; % Non-physical value to distinguish case of no
    % natural convection.
end
end

% Two cases: either calculations are made for some region, or they are not,
% since no relevant region exists (for the case of Nu_av = -1).

if Nu_av ~= -1;
    % Calculating S:
    S = (T_upper-T_lower)/(H*100);

    % Calculating isothermal Nu, isothermal temperature taken as LMTD:

    % Calculating LMTD for the configuration:
    LMTD_NC = (T_upper-T_lower)/log((T_upper-T_inf)/(T_lower-T_inf));

    % Calculating the Nusselt number for an isothermal case, the constant
    % wall temperature being T_inf+LMTD_NC (the latter calculated above).

    % Calculating film temperature:
    T_f_NC = T_inf+LMTD_NC/2;

    % Calculating air properties:
    beta = 1/T_f_NC;
    nu = 1/(2.4090e8/T_f_NC^(3/2)+2.6737e10/T_f_NC^(5/2));
    alpha = (-4.3274+4.1190e-2*T_f_NC+1.5556e-4*T_f_NC^2)*1e-6;

    % Calculating Pr, Gr and Ra:
    Pr = nu/beta;
    Gr = g*beta*LMTD_NC*H^3/(nu^2);
    Ra = Gr*Pr;

    % Calculating average Nusselt value for the isothermal plate:
    if Ra < 1e9;
        Nu_av_iso = 0.68+0.67*Ra^(1/4)/((1+(0.492/Pr)^(9/16))^(4/9));
    else
        Nu_av_iso = (0.825+0.387*Ra^(1/6)/...
            ((1+(0.492/Pr)^(9/16))^(8/27)))^2;
    end

    % Calculating average Nusselt value for the plate with linear wall
    % temperature profile, using literature formulas (Havet & Blay, 1999):
    if Ra > 2e9;
        Nu_av_NC = Nu_av_iso*(1+4.15*Ra^-0.15*S);
    else
        Nu_av_NC = Nu_av_iso*(1+0.17*S);
    end

    % Finding mean absolute percentage deviation between iteratively
    % calculated average Nusselt value and that calculated above:
    MAPD_Nu = sum(abs((Nu_av-Nu_av_NC)/Nu_av_NC*100));

else
    MAPD_Nu = -1; % Default value to distinguish case of no
    % natural convection.
end

```

end

end

Function TestMAPDNC

```
function [ MAPD_NC ] = TestMAPDNC( T_w, T_sup, T_ret, n )
% TestMAPD_NC: This function finds the mean absolute percentage deviation
% (MAPD) between the calculated T_w and the initially assumed completely
% linear temperature distribution along the surface.
%
% MAPD_NC: The mean absolute percentage deviation between T_w and the
% temperature distribution assumed initially.

% Calculating the originally assumed temperature distribution:
T_w_original = T_ret:(T_sup-T_ret)/n:T_sup;

% Calculating MAPD:
MAPD_NC = (1/n)*sum(abs((T_w-T_w_original)/...
    T_w_original)*100);

end
```

Function TestLinearity

```
function [ R_sqr_MLS, T_w_MLS_best_fit ] = TestLinearity( T_w, H, ...
    point_shift, n, CalcMode )
% TestLinearity: This function tests the linearity of a wall temperature
% distribution by using the Method of Least Squares (MLS). A linear fit is
% found, as well as coefficient of determination, R^2.
%
% The system of equations solved takes the form  $y = Ax$ , where a linear fit
% is found with form  $y = mx + c$ . (Note that this variables here have other
% meanings compared to elsewhere in the code.) Here,  $y = T_w$  and
%  $x = [m \ c]'$ .
%
% CalcMode: Variable determining which part of the plate is calculated.
% If CalcMode = 0, the case where calculations are made for the entire
% plate or its lower part.
% If CalcMode = 1, the part including point_shift and above is
% calculated.
%
% T_w_MLS_best_fit: The wall temperature distribution calculated using
% the best linear fit obtained.
%
% R_sqr_MLS: The coefficient of determination, R^2, for the linear fit
% found.

% Adjusting format of T_w:
if CalcMode == 0;
    T_w_adj = T_w(1:point_shift)';
else
```

```

    if point_shift ~= n+1;
        T_w_adj = T_w(point_shift:n)';
    else
        T_w_adj = -1; % Non-physical value to distinguish case of no
        % natural convection.
    end
end
end

% Two cases: either calculations are made for some region, or they are not,
% since no relevant region exists (for the case of T_w_adj = -1).

if T_w_adj ~= -1;
    % Creating a vector of y of length (n+1):
    if CalcMode == 0;
        if point_shift ~= n+1;
            y_relevant_points = [0:H/n:(point_shift-1)/n*H]';
        else
            y_relevant_points = [0:H/n:H]';
        end
    else
        y_relevant_points = [point_shift/n*H:H/n*H]';
    end

    % Creating a matrix A with coefficients m and c.
    A = [y_relevant_points ones(length(y_relevant_points),1)];

    % Solving the system of equations using MLS:
    x_MLS = A\T_w_adj;

    % Calculating the linear best-fit T_w:
    T_w_MLS_best_fit = A*x_MLS;

    % Calculating the R^2 for this:
    R_sqr_MLS = 1-sum((T_w_MLS_best_fit-T_w_adj).^2)/...
        sum((T_w_adj-mean(T_w_adj)).^2);
else
    R_sqr_MLS = -1;
    T_w_MLS_best_fit = -1; % Default values to distinguish cases of no
    % natural convection.
end

end

end

```

Function RadiativeHeatOutput

```

function [ Q_rad ] = RadiativeHeatOutput( T_w, T_inf, epsilon_rad, ...
    sigma, A_cell, LMTD_cell )
% RadiativeHeatOutput: This function calculates the radiative component of
% heat transfer from single cells.
%
% T_rad_mean: Mean radiating temperature. Based on assumption that
% surrounding surfaces have same temperature as the indoor temperature,
% T_inf.
%
% Q_rad: Radiative heat transfer from cell.

```

```

T_rad_mean =(((T_w(2:end)+T_w(1:(end-1)))/2+T_inf)/2+T_inf)/2;
Q_rad = 4*epsilon_rad*sigma*T_rad_mean.^3*A_cell.*LMTD_cell;

end

```

Function FindPointShift

```

function [ point_shift ] = FindPointShift( Ri, n )
% FindPointShift: This function is used in order to find the cell along the
% plate where the convection mode changes from forced or mixed to natural.
% Natural convection is considered to start where Ri > 10.
%
% point_shift: number of first calculation cell for which there is a
% transition to natural convection.

% Default value for point_shift, outside of range calculation cell index:
point_shift = n+1;

% Determining point shift:
for i = 1:n;
    if point_shift == n+1;
        if Ri(i) > 10;
            point_shift = i;
        end
    end
end
end

end

```

Function DimlessNumbers

```

function [ Pr, Gr, Ra, Re, Ri ] = DimlessNumbers( ny, alpha, g, beta, ...
    LMTD_acc, y_upper_bound, u )
% DimlessNumbers: Given constants and earlier calculated properties, this
% function returns relevant dimensionless numbers.
%
% Pr: Prandtl number.
%
% Gr: Grashof number.
%
% Ra: Rayleigh number.
%
% Re: Reynolds number.
%
% Ri: Richardson number.

Pr = ny./alpha;

Gr = g*beta.*LMTD_acc.*y_upper_bound.^3./(ny.^2);

Ra = Gr.*Pr;

```

```
Re = u*y_upper_bound./ny;
```

```
Ri = Gr./(Re.^2);
```

```
end
```

Function ConvectiveHeatOutput

```
function [ Nu_total_av, Nu_local_av, Q_con ] = ...
    ConvectiveHeatOutput( n, Ra, Pr, Re, Ri, y_upper_bound, lambda, ...
        y_mid, A_cell, LMTD_cell )
% ConvectiveHeatOutput: This function calculates the convective component
% of heat transfer from single cells.
%
% Nu_av_n: Average Nusselt number along a height for completely natural
% convection.
%
% Nu_av_f: Average Nusselt number along a height for completely forced
% convection.
%
% Nu_av: Average Nusselt number along a height, regardless of convection
% type.
%
% Nu_local_av: Average local Nusselt number for a cell.
%
% Nu_total_av: Total average Nusselt value - average Nusselt value along
% the entire plate.
%
% h_con: Convective heat transfer coefficient for a cell.
%
% Q_con: Convective heat output for a cell.

% Creating empty lists to fill:
Nu_av_n = zeros(1,n);
Nu_av_f = zeros(1,n);
Nu_av = zeros(1,n);
Nu_local_av = zeros(1,n);
h_con = zeros(1,n);
Q_con = zeros(1,n);

for i = 1:n;
    % Nusselt value for natural convection:
    if Ra(i) < 1e9;
        Nu_av_n(i) =
0.68+0.67*Ra(i)^(1/4)/((1+(0.492/Pr(i))^(9/16))^(4/9));
    else
        Nu_av_n(i) = (0.825+0.387*Ra(i)^(1/6)/((1+(0.492/Pr(i))^(...
(9/16))^(8/27)))^2;
    end

    % Nusselt value for forced convection:
    if Re(i) < 1e7;
        if Re(i) < 5e5;
            Nu_av_f(i) = 0.664*Re(i)^0.5*Pr(i)^(1/3);
        else
            Nu_av_f(i) = Pr(i)^(1/3)*(0.037*Re(i)^0.8-871);
        end
    end
end
```

```

        end
    else
        display('Error! Re out of range for forced convection.')
    end

    % Average Nusselt value:
    if Ri(i) > 10;
        Nu_av(i) = Nu_av_n(i);
    elseif Ri(i) < 0.01;
        Nu_av(i) = Nu_av_f(i);
    else
        Nu_av(i) = (Nu_av_n(i)^3+Nu_av_f(i)^3)^(1/3);
    end

    % Local Nusselt number:
    if i == 1;
        Nu_local_av(i) = Nu_av(i);
    else
        Nu_local_av(i) = (Nu_av(i)*y_upper_bound(i)-...
            Nu_av(i-1)*y_upper_bound(i-1))/(y_upper_bound(i)-...
            y_upper_bound(i-1));
    end

    % Total average Nusselt value:
    Nu_total_av = sum(Nu_local_av)/n;

    % Convective heat transfer coefficient:
    h_con(i) = Nu_local_av(i)*lambda(i)/y_mid(i);

    % Convective heat transfer:
    Q_con(i) = h_con(i)*A_cell*LMTD_cell(i);

end

end

```

Function CalcValuesUpdate

```

function [ Q_tot, T_w, max_change, T_ret, dT, C ] = ...
    CalcValuesUpdate( T_w, T_sup, T_ret, T_inf, C, Q_rad, Q_con, n, ...
        ConvectionMode )
% CalcValuesUpdate: This function marks the end of the iterative loop used
% for calculating total heat output. The function returns a new temperature
% profile, as well as other needed values.
%
% Q_tot: Total heat output of a cell.
%
% ConvectionMode: Input variable for different convection modes.
% If u = 0, ConvectionMode = 0
% If u > 0, ConvectionMode = 1
%
% C: Heat capacity rate, i e mass flow x fluid's specific heat capacity.
%
% max_change: the largest relative change between a cell's two
% temperatures between two iterations.

```

```

% Calculating total heat output:
Q_tot = Q_rad + Q_con;

% Saving old temperatures:
T_w_old = T_w;

% Defining dT:
dT = T_sup-T_ret;

% Changing dT when u > 0:
if ConvectionMode == 1;
    % T_ret is changed, as more heat is lost than for base case of u = 0.
    % New T_ret becomes:
    T_ret = T_sup-sum(Q_tot)/C;

    % Adjusting to acceptable value, to prevent calculation error:
    if T_ret <= T_inf;
        T_ret = T_inf+1e-1; % 1e-1 is arbitrary small adjustment
    end

    % The new temperature drop dT becomes:
    dT = T_sup-T_ret;
end

% Updating temperature profile:
for i = 1:n+1;
    T_w(i) = T_ret+(sum(Q_tot(1:i-1))/sum(Q_tot))*dT;
end

% Finding new largest relative change:
max_change = max(abs((T_w - T_w_old)./T_w_old));

% Updating heat capacity rate:
if ConvectionMode == 0;
    C = sum(Q_tot)/dT;
end

end

```

Function AirProperties

```

function [ lambda, beta, ny, alpha ] = AirProperties( T_f_local_av, ...
    T_f_acc_av )
% AirProperties: Given a specific wall temperature distribution, the
% function returns the air properties needed for further calculations.
%
% lambda: Thermal conductivity. Evaluated locally for every single cell.
%
% beta: Thermal expansion coefficient. Evaluated accumulatively along a
% height up to a certain point.
%
% ny: Kinematic viscosity. Evaluated accumulatively along a
% height up to a certain point.
%
% alpha: Thermal diffusivity. Evaluated accumulatively along a
% height up to a certain point.

```

```
lambda = 2.3340e-3*T_f_local_av.^(3/2)./(164.54+T_f_local_av);  
beta = 1./T_f_acc_av;  
ny = 1./(2.4090e8./T_f_acc_av.^(3/2)+2.6737e10./T_f_acc_av.^(5/2));  
alpha = (-4.3274+4.1190e-2*T_f_acc_av+1.5556e-4*T_f_acc_av.^2)*1e-6;  
end
```